

Active Volcanism on Io: Global Distribution and Variations in
Activity

Rosaly Lopes-Gautier¹, Alfred S. McEwen², William D. Smythe¹, P. E. Geissler², L. Kamp¹, A. G. Davies¹, J.R. Spencer³, L. Keszthelyi², R. Carlson¹, F.E. Leader⁴, R. Mehlman⁴, L. Soderblom⁵, and the Galileo NIMS and SSI Teams.

¹ Jet Propulsion Laboratory, California Institute of Technology, Pasadena, CA 91109, ² Lunar and Planetary Laboratory, University of Arizona, Tucson, ³ Lowell Observatory, Flagstaff, Arizona, ⁴ Institute of Geophysics and Planetary Physics, University of California, Los Angeles, ⁵ U.S. Geological Survey Branch of Astrogeology, Flagstaff, Arizona

Correspondence to: Rosaly Lopes-Gautier, Mail Stop 183-601, JPL
phone: (818) 393-4584
Fax: (818) 393-4605
E-mail: rlopes@issac.jpl.nasa.gov

45 pages, 5 tables, 11 figures

Key topics: Io, volcanology, heat flow

Proposed running title: Active Volcanism on Io

Abstract: Io's volcanic activity has been monitored by instruments aboard the Galileo spacecraft since June 28, 1996. We present results from observations by the Near-Infrared Mapping Spectrometer (NIMS) for the first ten orbits of Galileo, correlate them with results from the Solid State Imaging System (SSI) and from ground-based observations, and compare them to what was known about Io's volcanic activity from observations made during the two Voyager fly-bys in 1979. A total of 61 active volcanic centers have been identified from Voyager, ground-based, and Galileo observations. Of these, 41 are hot spots detected by NIMS and/or SSI. Another 25 locations were identified as possible active volcanic centers, mostly on the basis of observed surface changes. The distribution of active volcanic centers on the surface does not show any clear correlation with latitude, longitude, Voyager-derived global topography, or with heat flow patterns predicted by the asthenosphere and deep mantle tidal dissipation models. Hot spots are correlated with surface colors, particularly dark and red deposits, and generally anti-correlated with white, SO₂-rich areas. Surface features corresponding to the hot spots, mostly calderas or flows, were identified from Galileo and Voyager images. Hot spot temperatures obtained from both NIMS and SSI are consistent with silicate volcanism, which appears to be widespread on Io. Two types of hot spot activity are present: persistent-type activity, lasting from months to years, and sporadic events, which may represent either short-lived activity or low-level activity that occasionally flares up. Sporadic events are not often detected, but may make an important contribution to Io's heat flow and resurfacing.

Persistent hot spots and active plumes are concentrated towards lower latitudes and this distribution favors the asthenosphere rather than the deep mantle tidal dissipation model.

1. Introduction

One of the major objectives of the Galileo mission is to study Io's volcanic activity and how it varies with time. Active volcanism on Io was discovered from images and infra-red measurements taken by the Voyager 1 spacecraft during its flyby of the Jupiter system in 1979 [e.g. Smith et al. 1979]. Four months later, the Voyager 2 flyby revealed that some major changes had taken place on Io, including the apparent shut-off of the Pele plume and the filling of the fallout ring around Pele. Analysis of Voyager 1 IRIS data [Pearl and Sinton 1982, McEwen et al. 1992a, 1992b] showed at least 22 hot spots over about a third of the surface. The cameras (ISS) aboard the two Voyager spacecraft detected a total of 9 active plumes [Strom et al. 1981, McEwen et al. 1989]. All of the plume sites that were also observed by IRIS showed the presence of hot spots.

Since Voyager, Io's activity has been monitored by observations from ground-based telescopes [e.g. Veeder et al. 1994, Goguen et al. 1988, Spencer et al. 1997a]. Hot spot detections from ground-based observations were summarized by Spencer and Schneider [1996] and Spencer et al. [1997a].

The Galileo mission has provided the unprecedented opportunity to monitor the activity of Io's volcanoes from Jupiter orbit. During its two-year primary mission, from December 1995 to December 1997, Galileo has encountered Ganymede, Callisto, and Europa. The spacecraft has come no closer to Io than 120,000 km during each orbit, except at Jupiter Orbit Insertion (JOI) when no remote sensing observations were taken. Closer ranges are planned during

the Galileo Europa Mission (GEM), including two close fly-bys of Io at the end of the mission in 1999. The Near-Infrared Mapping Spectrometer (NIMS) has observed Io at least twice during each of Galileo's orbits, starting on June 28, 1996. The main objectives of the NIMS observations of Io are (i) to investigate the distribution and temporal variability of hot spots on Io's surface [Lopes-Gautier et al. 1997a] and (ii) to determine Io's surface composition and the distribution of SO₂ on the surface [Carlson et al. 1997].

The Solid State Imaging System (SSI) aboard Galileo is investigating Io's geologic features, plume activity, surface colors, and high-temperature hot spot activity [McEwen et al. 1997, 1998a,b; Carr et al. 1998, Simonelli et al. 1997; Geissler et al., *Icarus*, in press]. SSI's spatial resolution is 50 times that of NIMS, enabling it to detect smaller hot spots than NIMS can, as long as the temperatures of these hot spots are sufficiently high to be detectable using the camera. SSI can detect hot spots having a minimum temperature of 700 K if the pixel is filled [McEwen et al. 1997]. The NIMS wavelength range, from 0.7 to 5.2 micrometers, enables it to detect cooler hot spots than SSI, down to 180 K if the hot spot fills a NIMS pixel [Smythe et al. 1995]. All of the NIMS pixels in the observations obtained so far are greater than 14,884 km², significantly larger than hot spot areas, which are typically only a few square kilometers [Lopes-Gautier et al. 1997]. The coolest temperatures obtained from a single black-body fit to NIMS data have been about 300 K.

The combination of NIMS and SSI observations is of great value

for the study of Io's volcanic activity. The two instruments provide complementary data for investigating the relationship between hot spot activity, plume activity, and surface geology. We present here the results of the NIMS search for new and recurrent hot spots on Io from observations taken during Galileo's first ten orbits. We combine the NIMS results with those from the SSI observations [McEwen et al. 1997, 1998a], those from ground-based observations obtained during and prior to the Galileo mission [summarized in Spencer et al. 1997a], and those obtained from Voyager data [Pearl and Sinton 1982, McEwen et al. 1992a,b]. The combination of these data sets provides our most complete view to date of the global distribution and temporal variability of Io's hot spot activity.

2. Io Observations by Galileo NIMS and SSI

The NIMS instrument has been described previously by Carlson et al. [1992] and Smythe et al. [1995]. NIMS includes a spectrometer with a scanning grating and spans the wavelength range 0.7 to 5.2 micrometers, therefore measuring both reflected sunlight and thermal emission. NIMS forms spectra with 17 detectors in combination with a moving grating. The 17 wavelengths obtained for each grating position are acquired simultaneously, thus providing a "snapshot" spectrum of the target. Spectra obtained for different grating positions are not located precisely on the same spot on the planet, because of motion of the field of view relative to the surface during the time between grating steps (0.33 seconds). This motion has implications for the analysis of NIMS data, such as the

variance of hot spot temperatures measured [Lopes-Gautier et al. 1997].

NIMS has observed Io at least twice per orbit during Galileo's orbits G1 through C10, corresponding to the period from June 28, 1996 to September 20, 1997. Most observations were taken within one to three days of closest approach in each orbit, covering all latitudes and either the whole disk or part of the disk. The NIMS global coverage of Io in these orbits had spatial resolutions typically in the range 200-500 km/pixel. The highest spatial resolution was obtained on the anti-Jovian hemisphere (122 km/pixel), while the poorest spatial resolution was on the Jupiter-facing hemisphere (for the swath 350W-0-40W the resolution was, at best, 516 km/pixel). Often, NIMS has taken pairs of observations close together in time, one covering Io's dayside and the other Io's nightside, to permit a more sensitive gain state can be used for the nightside. Most observations are taken using from 102 to 408 wavelengths. A small number of NIMS Io observations taken during the first few orbits returned fewer than 102 wavelengths, and are harder to interpret. The high radiation environment near Jupiter causes noise spikes to be introduced in the data, which must be removed before data analysis. The higher the number of wavelengths returned, the easier it is to identify and remove the radiation-induced noise.

The Galileo SSI instrument has been described by Belton et al. [1992] and by Klaasen et al. [1997]. McEwen et al. [1998a] summarized observations taken during the first 10 orbits of Galileo and the major results from the observing campaign. Of particular

interest to this paper are SSI's eclipse observations, taken when Io is in Jupiter's shadow. Long-exposure images are taken to search for high-temperature hot spots and diffuse atmospheric/plume glows. Use of SSI's clear (CLR) and 1-micrometer (1MC) filters on the same observation allows hot spot temperatures to be estimated [McEwen et al. 1998b]. Eclipse observations were obtained by SSI in orbits G1, E4, E6, G7, G8, C9, and C10, and E11.

3. Detection of Hot Spots

The detection of hot spots by NIMS during the first four Galileo orbits (G1, G2, C3, and E4) was discussed by Lopes-Gautier et al. [1997a]. Here we update the previous study to include NIMS results from the Galileo orbits E6, G7, G8, C9, and C10.

The NIMS search for hot spots consists of a pixel-by-pixel analysis of each observation. A pixel is considered to contain a hot spot when the positive slope of the spectrum between 3.5 and 5 micrometers is greater than that of all surrounding pixels. However, the pixels identified as hot spots in this search do not account for all of the thermal emission that NIMS detects from Io, as discussed by Lopes-Gautier et al. [1997a]. A pixel-by-pixel thermal map of a NIMS observation of Io's nightside during the first orbit [Smythe et al. 1997] shows other NIMS pixels that have significant thermal output based on their increasing radiance from 3 to 5 micrometers. These pixels are not listed as pixels containing hot spots in our search because they fall in one of two categories. The first is when the thermal signal is relatively weak, that is, the local maximum is less than 5% greater than that

of the surrounding pixels. This probably represents hot spots that are relatively small or cool, and further analysis and/or independent measurements are needed before they can be identified as hot spots. In the second category are the cases where a pixel has a significant thermal signal between 3 and 5 micrometers, but the output is less than that from neighboring pixels which were identified as hot spots. This may represent adjacent hot spots that cannot be fully resolved at the available spatial resolution, or energy that is distributed between pixels because of the instrument's point-spread function [Carlson et al. 1992]. All temperature-area calculations done so far show that Io's hot spots are sub-pixel at NIMS spatial resolutions. Pixel-by-pixel thermal maps using the method explained by Smythe et al. [1997, 1999] will clarify the existence of hot spots in the two categories above. The hot spot detections given in this paper should, therefore, be considered as the minimum number of hot spots detectable from NIMS data. In terms of power output measured from NIMS nightside data [Lopes-Gautier et al. 1999], the majority of hot spots detected fall in the range 10^{10} to 10^{11} Watts.

The positions of hot spots observed by NIMS in orbits G1 through C10 are listed in Table 1. Also listed on Table 1 are: (i) positions of hot spots and plume sites detected from SSI eclipse data; (ii) positions of hot spots detected by Voyager IRIS and from ground-based observations and their possible correlation with NIMS and SSI hot spots; and (iii) positions and types of features on the surface that we infer to be the sources of the thermal emission detected by NIMS, SSI, IRIS, and ground-based observations. The hot

spot latitudes and longitudes obtained from NIMS data were determined from the highest spatial resolution observations available for each region. The coordinates are the central coordinates of the NIMS pixels containing each hot spot. Errors listed correspond to half a NIMS field of view (i.e. half the pixel size). The corresponding positions derived from SSI hot spot detections [McEwen et al. 1997, 1998a], when available, are more precise because of the higher spatial resolution of the camera. Errors in latitude and longitude for SSI hot spot positions are usually less than 1 degree [McEwen et al. 1997]. The positions of volcanic centers identified as the source areas for individual hot spots were taken from SSI images that show these surface features in detail. In all cases, these features are located within the error limits of the positions derived from NIMS data. The volcanic centers consist of calderas, flows, and/or plume deposits, and in every case show the presence of low-albedo material.

A total of 37 hot spots have been detected by NIMS, including 22 that were not known from Voyager or ground-based measurements. Most of these hot spots were detected by NIMS in the anti-Jovian hemisphere, which was observed by Voyager at low spatial resolution. The anti-Jovian hemisphere is also poorly observed from the ground, but it is where the NIMS spatial resolution is highest, due to the configuration of Galileo's orbits. SSI detected hot spots at 18 locations during orbits G1 through C10. This number is a minimum because (i) some bright pixels seen in SSI eclipse images have not yet been confirmed to be hot spots (Table 2) and (ii) the hot spots at three of these locations span multiple hot spots. For

the purpose of this analysis, we have treated the following multiple hot spot complexes as single volcanic centers: Kanehekili N&S, Isum N&S, Pillan and Pillan N&S. The reason is that most of the monitoring observations are from NIMS and so far it has not been possible to resolve the multiple components seen by SSI in the NIMS observations. Treating these as single volcanic centers simplifies the analysis. A total of 14 hot spots were detected by both NIMS and SSI, often in observations taken during different orbits.

Lack of detection of an SSI hot spot by NIMS is most likely due to 50 times lower spatial resolution of NIMS or else the temporal variability of some hot spots. An example of the latter is probably the Reiden hot spot detected by SSI during orbit G1. NIMS did not observe the Reiden Patera region during G1. However, observations in several other orbits, at resolutions down to 122 km/pixel, have failed to detect this hot spot, but have detected all others shown in the same SSI G1 image. Since Reiden has not been observed as a hot spot by SSI in later orbits, it is likely that the activity there either stopped after the G1 observation by SSI, or waned to levels below the sensitivity of either instrument. Alternatively, the SSI hot spot could have been spurious, although it is unlikely that noise would mimic the same shape as the smear ellipse.

Lack of detection of a NIMS hot spot by SSI is most likely due to the lack of a significant high temperature component (above 700 K), and hence of significant energy at 1 micrometer. These "cooler" hot spots include Hi'iaka, which was discovered from ground-based

observations [Spencer et al. 1997a] and Malik, first seen as a hot spot by NIMS in orbit G1.

A total of 61 active volcanic centers are listed in Table 1, plus two others that are hot spots identified from IRIS data, but have uncertainties large enough that more than one candidate site is listed (Mithra or Pyerun and Shakura or Daedalus). Table 2 lists an additional 25 sites that we consider likely to be active volcanic centers, but have yet to be confirmed. The activity at these sites is suggested by one or more of the following: (i) surface changes detected by comparing SSI and Voyager images; (ii) faint glow in an SSI eclipse image, which suggests a region of degassing or a faint hot spot, (iii) presence of reddish materials that are thought to be indicative of recent activity, (iv) presence of a plume-type deposit, (v) possible identification of a hot spot detected by ground-based observations, (vi) possible identification of a site where changes were reported by observations from the Hubble Space Telescope [Spencer et al. 1997b].

The identification of volcanic centers on the surface corresponding to hot spots detected by ground-based observations can be problematic because of the large uncertainties associated with the positions of hot spots in these observations. Table 3 lists observations by Spencer et al. [1997a] during 1996 and 1997, with possible identifications based on data from Voyager and Galileo. Surface locations for two outbursts observed on Io between Voyager and Galileo (summarized by Spencer and Schneider 1996) have been obtained. An outburst observed on November 6, 1979 [Sinton 1980] has a location consistent with Surt, while an outburst

detected on September 1, 1990 [Blaney et al. 1995] was most likely from Loki. Other reported outbursts have locations that are too uncertain for identification to be attempted, although Kanehekili would be consistent as the site of outbursts detected in 1986 and 1989 [Johnson et al. 1988, Veeder et al. 1994].

4. Distribution of hot spots on the surface

The hot spots detected by NIMS and SSI, together with hot spots observed from the ground by Spencer et al. [1997a] during 1995 and 1996 are shown superimposed on a global mosaic of SSI images of Io (Fig. 1). The "Galileo-era" view of the distribution of hot spots on Io can be compared with the "Voyager-era" view, on which hot spots detected from IRIS data are plotted. It is clear that many more hot spots are present on Io than was known from analysis of the limited-coverage Voyager IRIS data, which revealed 22 hot spots over about 30% of Io's surface. We note that Galileo has not detected activity at 10 of these 22 hot spots (Nusku, Mbali, Uta, Pyerun/Mithra, Viracocha, Ulgen, Aten, Mazda, Nemea, and Creidne). SSI detected surface changes at Aten and Creidne, perhaps due to activity occurring between Voyager and Galileo observations. The hot spot Ulgen may have been detected by NIMS, but even in the current highest resolution observations by NIMS, the pixel size is still too large to enable us to confidently distinguish it from the Babbar hot spot.

The locations of active volcanic centers listed in Table 1 can be used to search for possible correlations with latitude, longitude, or topography, which may have important implications for

the mechanism of heat dissipation on Io. The active volcanic centers used for the following analysis are from Table 1. Since two Voyager hot spots had uncertain identifications (Shakura/Daedalus and Mithra/Pyeron), we have included both possibilities in our analysis. Daedalus is known to be a hot spot from Galileo data, but Shakura and one of Mithra/Pyeron may be spurious data points.

4.1. Distribution with latitude and longitude

The distribution of active volcanic centers (from Table 1) shows no obvious correlation with latitude or longitude, as indicated in the histograms in Figure 2. This agrees with McEwen's [1995] earlier study from Voyager data. Carr et al. [1998] plotted the distribution of calderas and other surface features interpreted as volcanic centers and also concluded that the distribution was uniform, except for an apparently somewhat lower density at high latitudes. We note from Figure 2 that there is an apparently lower concentration of active volcanic centers between latitudes 20 S and 30 S, and 0 to 10 N, but the present data are not sufficient to establish whether these departures from an uniform distribution are significant.

A factor that needs to be taken into account when considering the Galileo data is the spacecraft viewing geometry. Hot spots at latitudes over 45 degrees are viewed by Galileo at lower spatial resolutions than the equatorial regions and are therefore likely to be harder to detect (the sub-spacecraft point of all NIMS observations and SSI eclipse observations is near the equator). In addition to lower resolution, there is the possible effect of

topography. For example, a lava lake in a caldera will be increasingly obscured by the caldera wall at higher emission angles. The obscuration will depend on the depth and the diameter of the caldera, and the emission angle. A more subtle topographic effect involves molten material at the bottom of incandescent cracks. Hot spots surrounded by extensive hot lava flows, or erupting high fire fountains, could be detected at higher emission angles.

In many NIMS observations, we have noticed that hot spots can be detected near Io's limb, indicating that the effect of viewing geometry (emission angle) may not be substantial. The emission angle for each pixel is defined as the angle between the observer (spacecraft) and the normal to a planitodetic surface. We have examined the viewing geometry effect in Figure 3, where data from five NIMS observations (between orbits G2 and E4) were plotted. These observations were all taken at spatial resolutions from 122 to 350 km/pixel. They were all taken in reflected sunlight, therefore we have estimated the 5 micrometer flux for individual hot spots by subtracting the 5 micrometer flux of a nearby "cold" pixel. While this is a crude method to obtain the flux for hot spots, because of possible differences in albedo between the hot spot and the "cold" pixel (which may still contain a small amount of thermal energy), it is satisfactory for assessing the effect of emission angle (and thus viewing geometry) on the brightness of hot spots in general. The effect of emission angle is partly illustrated by the changes in the flux of Prometheus and Pele, though it is likely that some temporal variation in the flux also

occurred. While emission angle clearly has an effect, Figure 3 also illustrates that the hot spots detected by NIMS are sufficiently bright that they can still be detected at high emission angles. There is no clear correlation between the number of hot spots detected by NIMS and emission angle.

We consider that it is unlikely that there is a large number of hot spots undetected by NIMS at high latitudes of comparable brightness to the hot spots shown in Figure 3. However, the detection of hotter material by both NIMS and SSI is probably more sensitive to the effect of small-scale topography (and hence emission angle). Hotter material is more likely to be located inside cracks rather than on the flow surface, and thus be obscured at high emission angles.

The distribution of active volcanic centers with longitude (Fig. 2) also appears uniform when all the hot spot detections by the different instruments are combined. NIMS observations have higher spatial resolution on the anti-Jovian hemisphere and this is reflected in the relatively low number of hot spots detected between longitudes of about 320 W and 30 W. SSI imaged these longitudes in eclipse several times during the Galileo tour [McEwen et al. 1998a], and Voyager IRIS obtained more complete coverage on the Jupiter-facing hemisphere, which is also the preferred hemisphere for ground-based observations. The complementary coverage of NIMS, SSI, and IRIS gives us confidence that we have a reasonable sample of the number of hot spots present at all longitudes. It is, however, possible that additional hot spots with temperatures below the SSI limit of 700 K are present on the

Jupiter-facing hemisphere, and have not been detected by NIMS due to poor spatial resolution at those longitudes. A possible departure from the apparently uniform distribution in longitude may be implied by the detection by SSI of a field of about 26 bright spots near the sub-Jovian point at ± 15 degrees latitude, ± 30 degrees longitude [McEwen et al. 1998a]. It is not clear from the current SSI images whether these are hot spots, excited gases concentrated near vents, or both. McEwen et al. [1998a] also reported a diffuse glow over this region, and over a region of similar size near the anti-Jovian point which may suggest that a similar field of bright spots is present there. NIMS has not detected a concentration of hot spots near the anti-Jovian point, even though the spatial resolution of NIMS is highest on that hemisphere. We cannot rule out that hot vents may exist near the anti-Jovian point that are simply too small in area to be detectable with the available measurements.

4.2. Distribution of active volcanic centers and relation to tidal heating models

Hot spots are manifestations of Io's mechanism of internal heating and heat transfer. Most of Io's heat flow is radiated at wavelengths longer than 10 micrometers (e.g. Veeder et al. 1994), beyond the range of what NIMS and SSI can observe. However, the distribution of hot spots on the surface seen by the two instruments is useful for constraining models of internal heating. If we assume that these hot spots represent the major pathways of magma to Io's surface, then they would geographically reflect the

distribution of the total heat flow.

Two major models have been proposed for the dissipation of tidal heating on Io. Both models assume that convection is the main mode of heat transfer within Io, but differ on where the tidal heating predominantly occurs [Segatz et al. 1988, Ross et al. 1990, Gaskell et al. 1988]. If heating occurs mainly in an asthenosphere about 100 km thick, convection should occur globally, with centers of upwelling and downwelling separated by a few hundred kilometers. In the second model, tidal heating occurs in the deep mantle and results in larger-scale convection, perhaps with a relatively small number of mantle plumes spaced widely apart. The deep mantle model predicts greater heat dissipation (and higher concentration of hot spots) towards the poles. It is likely that some tidal heating does occur both in the deep mantle and in the asthenosphere, thus a combination of the two models, such as the 2/3 asthenosphere and 1/3 mantle heating model [Ross et al. 1990, Schubert et al. 1998], may be the most realistic scenario. In this paper, we consider only the two end-member models, as the difference in the heat flow patterns at the surface predicted by these two models is the most pronounced and may be reflected in the distribution of volcanic centers.

An earlier attempt to use spacecraft data to distinguish between these models was made by Gaskell et al. [1988], using the shape and large-scale topography of Io determined from Voyager 1 images. They suggested that the broad topographic swells revealed in the global topography could be due to isostatic responses to thermal changes in the lithosphere-asthenosphere system. In the

simplest picture, increasing the heat flow converts the basal lithosphere into lower-density asthenosphere, resulting in isostatic uplift. Gaskell et al. argued that if large-scale topography is positively correlated with heat flow, then the global pattern of basins and swells suggests that tidal dissipation occurs mostly in the asthenosphere. McEwen [1995] found no correlation between Voyager-detected hot spots and topography, but argued that the distribution of SO₂-rich areas on the surface supported the asthenosphere model.

We can use the combined Galileo, Voyager, and other data on active volcanic centers on Io (Table 1) to re-examine the relation between active volcanic centers and topography. The best complete global topography of Io available to date is still the map by Gaskell et al. [1988] based on Voyager data. The distribution of active volcanic centers from Table 1 is plotted on Gaskell et al.'s topographic map in Fig. 4a. A plot of the number of active volcanic centers relative to the map's elevations and areas [Fig. 4b] fails to show any significant correlation between the locations of active volcanic centers and topography. We note, however, that the plot in Fig. 4b is skewed towards lower elevations, implying a possible (but not statistically significant from the available data) higher concentration of active volcanic centers at lower elevations. This is the opposite of what might be expected from the isostatic uplift from the asthenosphere tidal dissipation model.

More recent results on Io's topography from Thomas et al. [1998], obtained from limb measurements made by Galileo SSI, show some disagreement with Gaskell et al.'s map. For example, Thomas et

al. [1998] did not confirm the pattern of longitudinal swells inferred by Gaskell et al. [1988] and Ross et al. [1990], which was used to support the asthenosphere tidal dissipation model. It is clear that the relation between locations of active volcanic centers and topography needs to be re-examined once improved global topography becomes available.

The spatial separation between active volcanic centers may help to differentiate between the asthenosphere and deep mantle models [McEwen et al. 1998a]. In the asthenosphere model, hot spots are expected to be uniformly distributed on the surface, separated at intervals of several hundred kilometers, perhaps with a preference for low latitudes. In the deep-mantle model, the centers of upwelling are further apart, and we might expect to find concentrations of hot spots in regions that would be widely separated from one another. Our data from Table 1 shows that the spacing between major hot spots ranges from about 150 km to about 700 km, with most hot spots being separated by about 200-400 km. The distribution is therefore more consistent with the asthenosphere model, in agreement with the conclusions by McEwen et al. [1998a] and Carr et al. [1998] based on imaging data alone.

We can examine the overall spatial distribution of active volcanic centers on the surface in relation to the predicted heat flow surface patterns of the two major models. According to Ross et al. [1990], although heat transfer processes will "smear" the interior heating distributions by the time the thermal energy appears at the surface, the signatures should be evident in the surface heat flow and the location of volcanoes and hot spots. We

can test this prediction, in part, by plotting the distribution of active volcanic centers over the heat flow patterns (Fig. 5) predicted by the two major models [from Ross et al. 1990]. While the locations of the active volcanic centers do not appear to correlate well with the predicted heat flow patterns from either model, it is more consistent with the asthenospheric model because of the apparently uniform distribution of active volcanic centers with longitude and latitude.

Although the global distribution and typical separations of active volcanic centers on Io are consistent with the asthenosphere model, measurements of volcanic heat flow from individual hot spots at a range of wavelengths are needed for more conclusive evidence. Volcanic heat flow has been measured by NIMS in the 0.7 to 5.2 micrometer range. Thermal maps made from NIMS nightside data, using the method of Smythe et al. [1997, 1999] will be important for determining patterns of volcanic heat flow. To the extent that the volcanic heat flow at these wavelengths is correlated with total surface heat flow, these measurements may provide a stronger basis for discriminating between tidal dissipation models than the distribution of active volcanic centers.

5. Correlation between active volcanic centers and surface features

The location of enhanced thermal emission detected by both NIMS and SSI can be correlated with features on the surface imaged by SSI. Tables 1 and 2 show the correlation between active volcanic centers and features on the surface that we consider to be candidate vent regions. The latitudes and longitudes given are

approximately those of the center of the surface features. The most common surface feature is a patera (usually a caldera), but other features include flucti (flows) and fissure-like features. A sample of surface features is shown in Figure 6.

Io presents a variety of surface colors, which are described in detail by McEwen et al. [1998a] and Geissler et al. [*Icarus*, in press]. The relation between the active volcanic centers (Table 1) and surface colors is shown in Figure 7, a map of the four major color units on Io. Red and orange materials dominate the dark polar regions of Io and are found at lower latitudes in isolated bright deposits; yellow and yellow-green materials, and white and grey materials, are mostly found at low latitudes; and low albedo materials occur mostly in many small spots marking the locations of active calderas [Geissler et al., *Icarus*, in press]. SSI results [McEwen et al. 1998a, Geissler et al., *Icarus*, in press] have confirmed the suggestion from Voyager observations [Pearl and Sinton 1982, McEwen et al. 1995] that hot spots are associated with low-albedo materials. Note that the map in Figure 7 does not show all of the low-albedo features, since some are too small to be shown at the scale of the map.

5.1 Red deposits

Red deposits are commonly associated with hot spots [Spencer et al. 1997b; McEwen et al. 1998a, Geissler et al., *Icarus*, in press]. Most regions that present red materials have been identified as hot spots or regions of surface changes [Geissler et al., *Icarus*, in press]. The red deposits may be fallout from

plumes, possibly fine droplets that were rapidly quenched, as suggested by Moses and Nash [1991]. They appear to fade with time and their spectral properties (as revealed by HST and Galileo SSI observations) are consistent with metastable short-chain S_3/S_4 molecules mixed with elemental sulfur or other sulfurous materials [see summary by Spencer et al. 1997b]. NIMS observations obtained up to now cannot spatially resolve the red deposits except for those in the ring surrounding Pele. Carlson et al. [1997] reported the presence of a 1.25 micrometer absorption feature, which may be due to iron-containing minerals, nearly everywhere on Io's surface, but not on the red ring surrounding Pele. Carlson et al. suggested that the red deposits, which may be sulfur from plume fallout, could be covering the iron-containing deposits on the surface.

The inventory of hot spots and plume sites presented in Table 1 allows us to further investigate the correlation between red materials, hot spots, and plume sites. In Table 1, we have identified 59 hot spots from Voyager, Galileo, and ground-based data. Thirty-nine percent of these hot spots have red deposits associated with them (23/59). If red deposits are indeed the result of plume activity, this may possibly reflect a lower limit of how often plume and hot spot activity are associated.

Plume activity is perhaps only found at hot spots, but the reverse is probably not true. Plumes have not been detected at most hot spots, though they could occur sporadically. Long time intervals between plume activity, or very short durations, would make detection difficult. There are only two known plume sites where hot spots have so far not been detected: Ra, observed by SSI

in G1, and Masubi, observed by Voyager. The lack of detection of a hot spot at Masubi may well have been due to the poor resolution of IRIS at that location. Masubi may have faded since Voyager, as no plume or hot spot has been detected there by Galileo up to orbit C10. No hot spot has been detected at Ra by either NIMS or SSI, even though both instruments have viewed the location in several observations at different geometries. The lack of detection of a hot spot could be due to temporal variability, to relatively cool temperatures making it unlikely to be detected by SSI, and to the poor spatial resolution of NIMS at the longitude of Ra (325 W). Red deposits are not seen by Galileo SSI at either Masubi or Ra.

How well do plumes and red deposits correlate? Plumes have only been observed by SSI at 5 (6, if we include the marginal identification of a plume at Culann) of the 23 hot spots associated with red deposits (22 or 26%), but this is a higher occurrence than plumes observed by Galileo at hot spots not associated with red deposits (3 plumes detected at 36 hot spots, or 8%). We do not include Voyager observed plumes because red deposits cannot be identified reliably from Voyager ISS data [Geissler et al., *Icarus*, in press]. While it can be argued that red deposits are the result of plume activity, and that plumes were at one time present at the active volcanic centers now showing red deposits, it is clear that at least a few plumes have not produced red deposits. Bright white deposits surround some plumes sites (e.g. Prometheus) and may be produced by plumes containing pure SO₂. Diffuse dark deposits found at other sites (e.g. Pillan) may represent silicates in the plume.

What is the lifetime of red deposits? Observations by Spencer

et al. [1997b] using HST showed that the bright spot at Ra Patera persisted for longer than one year. If we postulate that red deposits, plume activity, and hot spots are associated, we can use the Galileo NIMS and SSI data to further constrain the lifetime of the red deposits. One striking example is Tohil Patera (at 26S, 158W), which is surrounded by red deposits. SSI has not detected a hot spot, plume, or surface change at Tohil during the Galileo mission. Voyager IRIS also did not detect a hot spot at Tohil, but this could easily be due to the poor spatial resolution of IRIS over this hemisphere. NIMS has observed this region at least once per orbit (except orbit E4), detecting hot spots at regions nearby (such as Shamash and Culann) but not at Tohil. While it cannot be ruled out that Tohil is a faint hot spot below the resolution limit of both NIMS and SSI, it can safely be said that Tohil has not had activity at a comparable level to that of other hot spots in the region since Galileo began observing in June 1996. It has possibly not been active at all during this time. The lack of activity would imply that the lifetime of the red deposits can be at least 18 months.

5.2. White deposits

Active volcanic centers are generally anti-correlated with large areas of bright white deposits. As Figure 7 shows, the surface of Io has large regions that are predominantly white and mostly occur at low latitudes. These regions were first seen on Voyager images and interpreted by Smith et al. [1979] to be rich in SO₂ frost or ice. NIMS spectral mapping from an observation that

included the bright white equatorial regions of Colchis Regio (centered at about 210 W) and part of Bosphorus Regio (centered at about 120 W) showed that these areas have extensive snowfields of SO₂ with larger particles (> 250 micrometers in diameter) beneath smaller particles, while the pervasive covering of SO₂ elsewhere has smaller characteristic grain sizes [Carlson et al. 1997].

The identification of higher concentrations of SO₂ frost in the bright white areas, which are anti-correlated with hot spots, is consistent with these areas being colder than the surrounding regions where hot spots are located. Volcanic activity supplies SO₂, which condenses in regional cold traps that sustain SO₂ snowfields, as discussed by Fanale et al. [1982] and Kerton et al. [1996]. A particularly good example of the anti-correlation between hot spots and bright white areas is Bosphorus Regio. Lopes-Gautier et al. [1997a] presented a NIMS 5-micrometer map from a nightside observation of Bosphorus Regio. The map shows that pixels located in the center of Bosphorus Regio (corresponding to the bright white area) have no detectable thermal signal, while the pixels located in surrounding Bosphorus Regio show significant thermal signal and form a hot spot "ring of fire".

While the anti-correlation between hot spots and cold SO₂ snowfields (bright white areas) is to be expected, it is not clear why the bright white areas occur geographically where they do. Voyager data suggest that SO₂ is concentrated in equatorial topographic basins [McEwen 1995]. However, as discussed previously, topography from SSI data has not confirmed the existence of these basins [Thomas et al. 1998].

6. Hot Spot Activity

A summary of Galileo's detections of hot spot activity in different orbits is given in Table 4. Lack of detection of a hot spot by SSI or NIMS does not necessarily mean that the hot spot was not active at the time of the observation, but rather that the level of activity was below the detection limits for the instruments. This could mean temperatures too low, or spatial extent too small, to be detectable by either instrument.

It is clear that the spatial resolution of NIMS observations is a strong factor in whether or not hot spots can be detected. Another factor is whether the observation is of Io's dayside or nightside, as the solar component masks faint hot spots. Figure 8 shows a plot of the highest resolution NIMS observation in each orbit against the number of hot spots detected in each of those observations. NIMS detected fewer hot spots in orbits G7 and G8, where the range to Io was largest, than in other orbits, particularly C3, the closest approach to Io during the G1-C10 period. Therefore, the gaps in hot spot detection by NIMS shown in Table 4 may not reflect halts in activity, but activity below the detection at the NIMS spatial resolutions at each particular orbit. More hot spot activity may be detected when pixel-by-pixel thermal maps of NIMS observation are completed.

The combination of NIMS, SSI, ground-based, and Voyager data show that some hot spots appear to be persistently active, while the activity at other hot spots may consist of sporadic or short-lived events.

6.1. Persistent hot spots:

An important and somewhat surprising result from the Galileo observations is that many of Io's hot spots are active over periods of time ranging from months to years. It was known from ground-based observations that Loki is a persistently active hot spot, and that a few others such as Kanehekili and Hi'iaka are often active. The Galileo observations show that numerous other hot spots on Io also fall into this category. Although the lack of continuous temporal coverage introduces some uncertainty on whether these hot spots were active between consecutive detections, the Galileo observations show that the activity at these hot spots was either continuous (a single eruption) or consisted of frequent, intermittent events.

The hot spot detections by Galileo are listed in Table 4. For each hot spot, we list whether they were observed by either NIMS or SSI in any given orbit from G1 through C10, whether they were detected by either instrument, and whether they had been previously detected by Voyager or ground-based observations. We do not include the following active volcanic centers in this temporal analysis: hot spots not detected by Galileo, plume activity, and the marginal detection of Karei by SSI. The total number of hot spots considered in Table 4 is therefore 40.

We note that 8 hot spots were active for periods of time ranging from 3 months to 1 year. These hot spots are Maui, 9606W, Volund, Fo, Sethlaus, Rata, Kurdalagon, 9611A, Babbar, and Amaterasu. A total of 22 hot spots were active over timescales longer than 1 year. Table 5 shows how often these 22 hot spots were

observed and detected by NIMS and SSI. For each hot spot, we give the percentage of the number of Galileo orbits in which it was detected, out of the number of Galileo orbits in which it was observed. Seven of the hot spots were detected in 100% of the orbits in which they were observed, showing that at least at these locations activity was most likely continuous. Of these 7 hot spots, 5 were detected by Voyager in 1979 (Pele, Marduk, Isum, and Amirani, and the Prometheus plume), Hi'iaka, Kanehekili, and possibly Mulungu were detected from ground-based observations in the years between Voyager and Galileo. It is likely that activity at these hot spots (and possibly others not observed by Voyager IRIS) has persisted over several years, and perhaps some of them have been continuously active during the 17 years between Voyager and Galileo.

Is there a correlation between persistency of hot spot activity and plumes? We find that most of the known plumes that are associated with hot spots (i.e. excluding Ra and Masubi) were observed at the most persistent hot spots listed in Table 5 (9/12 or 75%). The only plume sites which do not coincide with the hot spots in Table 5 are the Voyager-observed plumes Maui and Volund, and the Galileo-observed Acala. Of these, Acala is the only hot spot that was not observed to be active over timescales of at least 3 months. Red deposits are prominent at 50% of the persistent hot spots listed in Table 5.

While persistent, the level of activity at the hot spots in Table 5 can vary significantly from orbit to orbit. The major changes detected by NIMS have been at Malik, Loki, and Pillan.

Malik brightened between orbits G1 and G2, indicating an increase in temperature of at least 400 K (Lopes-Gautier et al. 1997b). Pillan brightened between orbits G7 and C9, accompanied by the appearance of a plume and a dramatic change in surface appearance observed by SSI [McEwen et al. 1998a]. The Loki brightening between E6 and G7 was first reported by Spencer et al. [1997a] from ground-based observations. The brightening was clearly seen in a comparison between NIMS images from E6 and G7 (Fig. 9). In G7, NIMS observed Loki in darkness. NIMS data taken on Io's nightside was fit to a Planck function to yield a best-fit black body temperature for the spectra from each pixel (see Lopes-Gautier et al. 1997a and Davies et al. 1997 for a description of the method). The temperature and area obtained were compared to the ground-based measurements (Figure 10), indicating good agreement.

Less dramatic changes in activity were also observed by NIMS for other hot spots [Lopes-Gautier et al. 1999], with some hot spots brightening in terms of power output (e.g. Tupan between G1 and C9) and some fading (e.g. Altjirra from G1 to E11). It is possible that there are overall trends of brightening and fading for all of Io's persistent hot spots and these may be revealed by further analysis of NIMS data from all orbits.

6.2 Sporadic events

Hot spots that were detected less often than those in the persistent category may represent sites of sporadic, short-lived events. Alternatively, these hot spots may also be persistently active, but their activity may normally be at lower levels than can

be detected by the majority of our observations. We have found 9 hot spots observed by Galileo that are in this category. The observed activity at these 9 hot spots has lasted under 3 months. In the case of the Reiden hot spot that was only detected in the first orbit, G1, there is uncertainty to the duration of the active phase, because activity during the previous months was not known. Similarly, the duration of activity for hot spots only detected in C10 cannot be constrained until analysis of later orbits is done. These hot spots are Shamsu, (3N, 76W), and S. Sigurd.

The 5 hot spots where activity may indeed have been short-lived are: the SSI-detected hot spot at (65N, 141W), Lei-Kung, Svarog, Daedalus, and Acala. Svarog, Daedalus, and Acala were detected by Voyager IRIS, therefore we know that activity at those sites re-occurs over timescales of years, even if individual events are short lived. It is likely that the single NIMS detection of Lei-Kung reflects normally low levels of activity rather than short duration, because Lei-Kung was detected only during the highest resolution observation by NIMS. Observations by NIMS at equal or higher spatial resolution, planned during GEM, will better constrain the nature of this hot spot. SSI observations of hot spots are likely to show more variation than those by NIMS, because SSI detects only the hotter material (> 700 K) from freshly-emplaced lavas. This material is more temporally variable than the lower temperature materials, from cooling lavas, that can be detected by NIMS.

While at most 5 of the Galileo-observed hot spots could be characterized as sporadic events, several of the hot spots detected

from the ground by Spencer et al. during the Galileo monitoring phase (Table 3) appear to be short-lived events. Galileo has not detected at least 9 of these ground-observed hot spots (see Tables 1 and 3). Three of these 9 hot spots were observed by Spencer et al. prior to the start of the main Galileo monitoring campaign on June 28, 1996, and six were observed during the Galileo campaign.

The 9503A event was an outburst and the hot spot persisted for several months. Outbursts are rare events [Spencer and Schneider 1996] and should be considered separately from either long-lived or sporadic activity. For the purposes of this analysis, we do not include 9503A as a sporadic event since it was observed more than once by Spencer et al. [1997a] over a period of several months. The 9507A and 9508A events were also observed more than once from the ground, and 9608A is possibly the same hot spot as 9508A. We consider the other 5 hot spots (9606E, 9606F, 9606G, 9606J, 9610A) to be possible sporadic events.

The hot spots 9606E, F, G, and J were observed on June 2, 1996. NIMS and SSI observed Io on June 28 and 29, but the observations did not cover the longitudes of these hot spots. The first opportunity Galileo had to detect 9606E, G, and J was during a NIMS observation taken in orbit G2 on September 7, 1996. The first Galileo observation of the 9606F location was an eclipse image taken by SSI during orbit E4 on December 17, during which the longitudes of 9606E, F, and G were also observed. We can infer that the activity of 9606E, G, and J waned to levels below detection by NIMS and SSI in 3 months or less, while the activity at 9606F waned in 6 months or less. Because of the lack of Galileo observations

prior to June 2, 1996, constraints on the total duration of activity at these hot spots cannot be obtained from Galileo data. Therefore, it is not clear that these are sporadic events according to our definition. However, lack of detection by Galileo during subsequent orbits, and by ground-based observations at any other time, implies that they may indeed have been short-lived.

Only one hot spot, 9610A, was detected from the ground between Galileo orbits. Limits on the duration of activity of this hot spot (at least at levels that can be detected by Galileo) can be obtained by using the dates of the Galileo observations. 9610A was observed from the ground on October 1, 1996. NIMS observations covering the same longitude taken on June 28, 1996, and on April 3, 1997, failed to show the hot spot, as did an SSI eclipse observation on December 17, 1996. The duration of the activity was therefore under 6 months. However, the high latitude of 9610A (70 ± 15) makes it somewhat less likely to be detected than low latitude events. It is possible that the hot spot persisted for longer, but the activity detected by Spencer et al. corresponded to a phase when high fire fountains were active, thus making the event possible to detect by observations which are essentially equatorial [Stansberry et al. 1997].

The fact that 5 possible sporadic events were detected by ground-based observations, compared with the same number observed by Galileo, stresses the importance of ground-based observations to monitor Io's activity. It is clear that understanding the frequency and magnitude of sporadic events is essential for our understanding of Io volcanism, and that can only be accomplished by frequent

monitoring. Once the Galileo mission is over, ground-based observations will be the primary remaining resource for continuing to build our knowledge of the frequency of sporadic events.

7. Summary, conclusions and future work

The comparison between Galileo NIMS and SSI data from nine Galileo orbits with those taken from ground-based telescopes and by Voyager IRIS has revealed new insights into Io's global distribution of volcanism, the correlation of hot spots with surface features, and the temporal behavior of hot spots. Below we discuss our findings and what they may imply to Io's heat flow models.

(i) Hot spots and surface features

The comparison of hot spot locations with surface features has shown that nearly all hot spots are associated with low-albedo features. This correlation had already been reported from SSI data [McEwen et al. 1998a, Carr et al. 1998, Geissler et al., *Icarus*, in press]. Here we find that it also holds for additional hot spots. The most common surface feature associated with active volcanic centers detected by NIMS and SSI is called a patera (usually a caldera), but others include flucti, and fissure-like features.

Carr et al.'s [1998] identification of volcanic centers based on morphology and albedo may provide an important tool for assessing the number and distribution of "sporadic" type hot spots, if we assume that the volcanic centers not yet identified as hot spots are sites of sporadic events. The size and morphology of

surface features still need to be correlated with hot spot type based on their temporal behavior (persistent or sporadic), and temperatures measured by NIMS and SSI.

(ii) Hot spots, plume activity, and red deposits

Our analysis supports the conclusions of Spencer et al. [1997b], McEwen et al. [1998a] and Geissler et al. [*Icarus*, in press] that red deposits are associated with active volcanic centers and are possibly the fallout from plumes. We find that 39% of known hot spots have red deposits associated with them. Active plumes have been observed by Galileo at 22 to 26% of these hot spots, and at only 8% of the hot spots not associated with red deposits. While it is plausible that plumes were at one time active at all the hot spots currently showing red deposits, it is also clear that a few plumes have not produced red deposits.

Red deposits are thought to be transient and to fade with time. Our analysis shows that red deposits are seen at some sites where no volcanic activity has been detected by Galileo, notably at Tohil Patera, which has been observed often by NIMS at the highest spatial resolution obtainable during the main Galileo mission. The lack of activity indicates that red deposits last for at least 18 months.

(iii) Hot spots and SO₂-rich regions

Hot spots are generally anti-correlated with bright white deposits, which are known to be regions of high concentrations of SO₂ frost and low temperatures [e.g. Carlson et al. 1997]. A

particularly striking example of this anti-correlation is Bosphorus Regio, which a NIMS thermal map shows to be a cold region surrounded by a ring of hot spots. While the anti-correlation between hot spots and cold SO₂ snowfields is expected, and supports the regional cold-trap model of Fanale et al. [1982], the geographical distribution of the snowfields has yet to be explained. Galileo SSI results [Thomas et al. 1998] do not support the existence of equatorial basins suggested from Voyager data [Gaskell et al. 1988, McEwen 1995], which were interpreted from Voyager to be SO₂-rich. Future work involving global thermal maps from NIMS data and a global topographic map from SSI data should clarify if the cold, bright white regions and local concentrations of hot spots (such as that around Bosphorus Regio) reflect the distribution of internal heating. It is also possible that the distribution of hot spots and cold regions reflect local differences in crustal thickness [Ross et al. 1990].

(iv) Temporal behavior of hot spots

Io's hot spots can be persistently active over timescales of months to years. Our results show that 8 hot spots were active over timescales of 3 months to at least one year, while the activity at 22 hot spots lasted for longer than one year, possibly much longer. Sporadic events also occur, and may represent short-lived activity or activity that is mostly at levels below the detection limits of the instruments. The contribution of these two types of activity to Io's global volcanism has yet to be assessed. Galileo data show that 5 hot spots may have been sporadic, while ground-based

observations reveal 5 other hot spots that may also fall in this category.

It is possible that all hot spots on Io are long-lived, but activity at the "sporadic" sites is normally at levels sufficiently low so that they cannot be detected by Galileo's instruments. Since activity at a hot spot may always be present at levels below detection, it is not practical to attempt to differentiate between the two categories of hot spots in terms of *actual duration of all activity*. However, the two types of hot spots are clearly different in terms of *duration of the vigorous active phase that can be detected by Galileo*. An important question is whether the "persistent" (or vigorous) and "sporadic" (short-lived or normally low-level) types of activity imply different types of volcanoes on Io, perhaps in terms of rate of magma supply, internal plumbing, or magma composition. If so, morphological differences may be present, but these are hard to characterize at present because of the small number of "sporadic" type hot spots known.

An important question raised by the temporal behavior of hot spots is: since levels of activity at all hot spots can fall to levels that cannot be detected by the currently available instruments, how many more active hot spots are there on Io? Would their number and distribution significantly change our current results?

Although the hot spots in the "persistent" category are clearly more likely to have been detected in the current data set than hot spots in the "sporadic" category, it is doubtful that we have detected all of the persistent hot spots. Apart from

constraints imposed by the relatively short duration of Galileo's monitoring phase and by the wavelength range of the instruments, there are also observational constraints. The bulk of the Galileo monitoring observations were carried out by NIMS, and NIMS observations had particularly low spatial resolution from longitudes 350W-0-40W. Therefore, it is not surprising that no "persistent" hot spots were observed within those longitudes. It is thus possible that a greater number of hot spots in this category are present close to the sub-Jovian point.

"Sporadic" events are clearly less likely to be detected, either because of their short duration or because the activity is at normally at low levels and only occasionally flares up. An important conclusion drawn from the temporal analysis is that these "sporadic" events do occur on Io, and can go largely undetected because the frequency of monitoring has been mostly on the scale of several months. The distribution of the "sporadic" hot spots is therefore largely unknown, as is their relative contribution to Io's heat flow. The conclusions drawn from our current set of observations are based largely on the distribution of persistent-type hot spots.

(vi) Implication of temporal behavior of hot spots to global distribution and to Io's heat flow

The combination of NIMS, SSI, ground-based, and Voyager IRIS data shows that there are at least 61 hot spots on Io, plus 2 plume sites where no hot spot has yet been detected. An additional 25 probable active volcanic centers were identified on the basis of

surface deposits, surface changes, or possible identification by ground-based or Hubble Space Telescope observations. Galileo observations have shown many more hot spots on Io than was known from the limited coverage of Voyager IRIS or from ground-based data, though it is likely that numerous other hot spots remain to be found.

It is important to note that NIMS and SSI cannot detect relatively low-temperature hot spots (below about 200 K) that may make an important contribution to the dissipation of Io's internal heat. It is not, however, unreasonable to assume that the heat flow distribution at Io's surface may be proportional to the heat flow detected by NIMS and SSI. Therefore, the hot spots detected by these instruments, plus those detected by Voyager and ground-based observations, may well reflect the first-order, overall distribution of heat flow on Io's surface. As Ross et al. [1990] stated, "although heat transfer processes will "smear" the interior heating distributions by the time the thermal energy appears at the surface, the signatures should be evident in the surface heat flow and locations of volcanoes and hot spots".

Our analysis shows that the distribution of active volcanic centers (hot spots plus two plumes sites) appears to be fairly uniform with respect to latitude and longitude. No correlation with global topography (derived from Voyager data) has been found, but this result will need to be re-examined when improved models of topography become available. The global distribution of all detected active volcanic centers is not well correlated with predictions of surface heat flow patterns derived from the

asthenosphere and deep mantle tidal dissipation models [Segatz et al. 1988, Ross et al. 1990]. The typical separations between active volcanic centers and the apparent deficit of centers at high latitudes are consistent with the asthenosphere model.

We can further examine how the distribution of active volcanic centers may reflect internal heating mechanisms by taking into account the differences between the volcanic centers. The most obvious differences are (i) power output of hot spots, (ii) presence of plumes, and (iii) persistency of activity. The effect of the first factor, power output, on the global distribution of hot spots is being examined by Smythe et al. [1999]. We note here that the overall distribution of hot spots is not necessarily correlated with the distribution of power output on the surface. For example, the output from Loki has been much higher than that measured at any other hot spot.

The second factor, presence of plumes, can be examined using data primarily from Galileo SSI. A series of plume monitoring observations have been conducted by SSI [McEwen et al. 1998a] and results showed that active plumes are indeed concentrated towards the equatorial regions. The third factor, persistency of activity, can be examined using the data presented in this paper. Figure 11 shows the distribution of hot spots overlaid on the heat flow pattern predicted by the asthenosphere tidal heating model, with the locations of plumes and persistent hot spots highlighted. It is clear that both plumes and persistent hot spots are concentrated towards lower latitudes. All persistent hot spots are located at latitudes lower than 50 degrees, in regions where the predicted

heat flow on the surface is greater than 1 W m^2 .

This result provides added support for the asthenosphere model, because persistent hot spots are likely to represent the current major pathways of magma from Io's interior to the surface. The predominance of plumes near the equator could reflect a correlation between plumes and persistent hot spots, but may also be an independent sign of vigorous, persistent activity on Io occurring mainly at lower latitudes. However, our results on the distribution of known hot spots can only provide strong evidence favoring a particular model if we accept the premise that the hot spots detected by Galileo, ground-based instruments, and Voyager IRIS are representative of the global distribution of all hot spots on Io, including low temperature thermal anomalies.

(v) Persistent hot spots

Galileo's long-term monitoring of hot spots can reveal possible differences among persistent hot spots, and changes in their levels of activity, that are important for characterizing Io's predominant eruption mechanisms.

SSI and NIMS are able to detect different phases (or possibly different types) of hot spot activity. Both instruments are able to detect bright, high-temperature hot spots such as Pele and Pillan. These are sites of very vigorous activity where a hot component is being frequently exposed at the surface. Possible scenarios include an overturning lava lake, or vents where a fresh supply of hot magma is being continuously fed to the surface. High temperatures measured at several of these hot spots, such as Pillan [McEwen et

al. 1998b], imply that the magmas are ultramafic in composition, possibly analogous to terrestrial komatiites. Our knowledge of the eruption processes of komatiites is limited because these eruptions komatiites have not occurred on Earth since the Archean. One important consideration for modeling the emplacement of lava flows on Io is that terrestrial komatiites are thought to have been emplaced as turbulent flows [Huppert et al. 1987; Huppert and Sparks 1985]. The majority of current lava flow emplacement models are based on the behavior of laminar flow.

The longer wavelength range of NIMS compared to SSI allows it to detect lower temperature hot spots. The "cooler" hot spots detected only by NIMS (e.g. Hi'iaka and Sigurd) may represent a type or stage of activity in which a high-temperature component (above 700 K) is either small in area or absent. This could be the case for a lava lake or flow that has a relatively cool crust over large parts of its area. Alternatively, it is possible that the magma being erupted at these hot spots is lower in temperature, perhaps implying different composition. We expect to be able to clarify these possibilities by doing more detailed analysis of the shorter wavelength data in the NIMS spectra. For example, fitting 2 or 3 temperatures to NIMS spectra [e.g. McEwen et al. 1998; Davies et al., *Icarus*, submitted] can reveal high temperature components of individual hot spots, provided the area is sufficiently large to be detected at NIMS spatial resolutions. Further measurements by SSI will also search for hot components at different times over the Galileo observing period. If high temperatures consistent with ultramafic volcanism are widespread on

Io, then the crust could be mafic. If high temperature volcanism is relatively rare, then Io's crust could be more evolved.

Significant variations in the level of activity of Io's "persistent" hot spots are known to occur. For example, dramatic variations in hot spot activity at Loki have been long known from ground-based data. Future detailed analysis of Galileo's numerous observations of "persistent" hot spots may reveal brightening and waning patterns that may be indicative of temporal changes in the rate of magma supply.

Understanding the behavior of persistent-type hot spots, including their overall eruption rates, can give us a window into the mechanisms involved in the transfer of magma from Io's interior to the surface. It is known that long-lived eruptions on Earth can last for decades [e.g. Simkin and Siebert 1994]. Recent examples for which the infra-red signature is well-documented include the 1983 to present eruption of Pu'u O'o in Hawaii, dominated by numerous lava flows [e.g. Flynn and Mouginis-Mark 1992] and the 1984 to 1995 eruption from a dome within the active crater of Lascar, Chile [Wooster and Rothery 1997]. Much longer timescales of volcanic activity are known on Earth, up to the 2,500 years of nearly-continuous activity at Stromboli. "Steady-state" volcanism on Earth occurs when the magma eruption rate is balanced by the magma supply rate. Therefore, measurements of the magma eruption rate can be used to estimate the minimum magma supply rate [e.g. Sigurdsson and MacDonald 1999, Harris et al. 1999, Oppenheimer and Francis, 1997]. Future work will take advantage of the many observations obtained by NIMS of persistent hot spots to measure

temporal variations in temperature and area, from which a range of eruption rates can be calculated using plausible thicknesses. These values can then be used to estimate the minimum magma supply rate to the surface at the present state of Io's volcanism.

(vii) Future observations

Further observations by Galileo during the Galileo Europa Mission (1998-2000) and from ground-based telescopes will continue to build up our knowledge of the types and temporal variability of hot spots on Io. Since Galileo will make few observations of Io during most of GEM, ground-based observations will continue to be essential for continuing the study of the temporal variability of Io's hot spots. Galileo will obtain very high spatial resolution observations of Io at the end of GEM (down to 200 m/pixel for NIMS and about 5 m/pixel for SSI). Areas targeted include inferred locations of volcanic throats, active plumes, and samples of red and dark materials. Although the temporal coverage will be small, these Galileo observations will, for the first time, show details of the morphology, thermal structure and composition of Io's active volcanic centers.

ACKNOWLEDGMENTS: We thank Robert Howell and David Rothery for helpful reviews; Elias Barbinis, Marcia Segura, Jim Shirley, Paul Herrera, and the Galileo team at JPL for support with sequencing and data downlink activities. Our work has greatly benefitted from discussions with other members of the ad-hoc Io Working Group. The

Galileo Project is funded by the Nasa Solar System Exploration Division. The work described here was performed at the Jet Propulsion Laboratory, California Institute of Technology, under contract with NASA.

REFERENCES:

Belton, M. J. S., and 22 colleagues 1992: The Galileo Solid State Imaging Experiment. *Space Sci. Rev.* **60**, 413-456.

Blaney, D. L., T. V. Johnson, D. L. Matson, and G. J. Veeder 1995. Volcanic eruptions on Io: Heat flow, resurfacing, and lava composition. *Icarus* **113**, 220-225.

Carlson, R. W., P. R. Weissman, W. D. Smythe, J. C. Mahoney, and the NIMS Science and Engineering Teams 1992. Near Infrared Spectrometer Experiment on Galileo. *Space Sci. Rev.* **60**, 457-502.

Carlson, R. W., W. D. Smythe, R. Lopes-Gautier, A. G. Davies, L. W. Kamp, J. A. Mosher, L. A. Soderblom, F. E. Leader, R. Mehlman, R. N. Clark, and F. P. Fanale 1997. The Distribution of Sulfur Dioxide and Other Infrared Absorbers on the Surface of Io in 1997. *Geophys. Res. Lett.* **24**, 2479-2482.

Carr, M. H., A. S. McEwen, K. A. Howard, F. C. Chuang, P. Thomas, P. Schuster, J. Oberst, G. Neukum, G. Schubert, and the Galileo Imaging Team 1998. Mountains and calderas on Io: Possible implications for lithosphere structure and magma generation. *Icarus* **135**, 146-165.

Davies, A. G., A. S. McEwen, R. Lopes-Gautier, L. Keszthelyi, R. W. Carlson, and W. D. Smythe 1997. Temperature and Area Constraints of

the S. Volund Volcano on Io from the NIMS and SSI instruments during the Galileo G1 orbit. *Geophys. Res. Lett.* **24**, 2447-2450.

Davies, A. G., R. Lopes-Gautier, W. D. Smythe, R. W. Carlson. Multiple-temperature fits to Galileo NIMS data of volcanism on Io. *Icarus*, submitted.

Fanale, F. P., W. P. Banerdt, L. S. Elson, T. V. Johnson, and R. W. Zurek 1982. Io's surface: its phase composition and influence on Io's atmosphere and Jupiter's magnetosphere. In *Satellites of Jupiter* (D. Morrison, Ed.), pp. 756-781, Univ. of Arizona Press, Tucson.

Flynn, L. P. and P.J. Mouginis-Mark 1992. Cooling rate of an active Hawaiian flow from nighttime spectroradiometer measurements. *J. Geophys. Res.* **19**, 1783-1786.

Gaskell R. W., S. P. Synnott, A. S. McEwen and G. G. Schaber 1988. Large-scale topography of Io: implications for internal structure and heat transfer. *Geophys. Res. Lett.* **15**, 581-584.

Geissler, P. E., A. S. McEwen, L. Keszthelyi, R. Lopes-Gautier, J. Granahan, D. P. Simonelli. Global color variations on Io. *Icarus*, in press.

Goguen, J. D., W. M. Sinton, D. L. Matson, R.R. Howell, H. M. Dyck, T. V. Johnson, R. H. Brown, G. J. Veeder, A. L. Lane, R. M. Nelson,

and R. A. McLaren 1988. Io's hot spots: infrared photometry of satellite occultations. *Icarus* 76, 465-484.

Harris, A. J. L., L. P. Flynn, D. A. Rothery, C. Oppenheimer, and S. B. Sherman 1999. Mass flux measurements at active lava lakes: implications for magma recycling. *J. Geophys. Res.*, in press.

Howell, R. 1997. Thermal emission from lava flows on Io. *Icarus*, 127 394-407.

Johnson, T. V., G. J. Veeder, D. L. Matson, R. H. Brown, R. M. Nelson, and D. Morrison 1988. Io: Evidence for silicate volcanism in 1986. *Science* 242, 1280-1283.

Kerton, C. R., F. P. Fanale, and J. R. Salvail 1996. The state of SO₂ on Io's surface. *J. Geophys. Res.* 101, 7555-7563.

Klaasen, K. P., and 15 colleagues. 1997. Inflight performance characteristics, calibration, and utilization of the Galileo SSI camera. *Opt. Eng.* 38, 3001-3027.

Lopes-Gautier, R., A. G. Davies, R. Carlson, W. Smythe, L. Kamp, L. Soderblom, F. E. Leader, R. Mehlman, and the Galileo NIMS Team 1997a. Hot Spots on Io: Initial Results from the Galileo Near-Infrared Mapping Spectrometer. *Geophys. Res. Lett.* 24, 2439-2442.

Lopes-Gautier, R., A. G. Davies, R. Carlson, W. Smythe, and L.

Soderblom 1997b. Monitoring of Io's Volcanic Activity using Galileo's Near Infrared Mapping Spectrometer (NIMS). *Lunar Planet. Sci.* XXVIII, pp. 831.

Lopes-Gautier, R., W. D. Smythe, A. S. McEwen, P. E. Geissler, A. G. Davies, L. Kamp, L. A. Soderblom, R. W. Carlson, L. Keszthelyi, J. R. Spencer, and the Galileo NIMS Team 1999. The Temporal Activity of Io's Hot Spots. *Lunar Planet. Sci.* XXX (available on CD-Rom).

McEwen, A. S. 1995. SO₂-Rich Equatorial Basins and Epeirogeny of Io. *Icarus* 113, p. 415-422.

McEwen, A. S., J. I. Lunine, and M. H. Carr 1989. Dynamic Geophysics of Io. In *Time-Variable Phenomena in the Jovian System* (M.J.S. Belton, R. A. West, J. Rahe, Eds), pp. 11-46. NASA S-P 494, Washington, DC.

McEwen, A. S., N. R. Isbell, and J. C. Pearl. 1992a. Io thermophysics: New models with Voyager 1 thermal IR spectra. *Lunar Planet. Sci.* XXIII, p. 881.

McEwen, A. S., N. R. Isbell, K. E. Edwards, and J. C. Pearl. 1992b. New Voyager 1 Hot Spot Identifications and the Heat Flow of Io. *Bull. Am. Astron. Soc.* 24, 935.

McEwen, A. S., D. Simonelli, D. Senske, K. Klaasen, L. Keszthelyi, T. Johnson, P. Geissler, M. Carr, and M. Belton 1997. High temperature hot spots on Io as seen by Galileo's Solid State Imaging (SSI) Experiment. *Geophys. Res. Lett.* **24**, 2443-2446.

McEwen, A. S., and 13 colleagues 1998a: Active volcanism on Io as seen by Galileo SSI. *Icarus* **135**, 181-219.

McEwen, A.S., and 14 colleagues 1998b: High temperature silicate volcanism on Jupiter's moon Io. *Science* **281**, 87-90.

Moses, J.I., and D. B. Nash 1991. Phase transformations and spectral reflectance of solid sulfur: Can metastable sulfur allotropes exist on Io? *Icarus* **89**, 277-304.

Oppenheimer, C. and P. Francis 1997. Remote sensing of heat, lava, and fumarole emissions from Erta'Ale volcano, Ethiopia. *Int. J. Remote Sensing* **98**, 4269-4286.

Pearl, J. and W. M. Sinton 1982. Hot Spots of Io. *In Satellites of Jupiter* (D. Morrison, Ed.), pp. 724-755, Univ. Ariz. Press, Tucson.

Ross, M. N., G. Schubert, T. Spohn, and R. W. Gaskell 1990. Internal structure of Io and the global distribution of its topography. *Icarus* **85**, 309-325.

Schubert, G., P. J. Tackley, J. P. Matas, G. A. Glatzmaier, and J.

T. Ratcliff 1998. Three-Dimensional Numerical Simulations of Mantle Convection in Io. *Eos* (Fall Supplement) 79, p. F529.

Segatz, M., T. Spohn, M. N. Ross, and G. Schubert 1988. Tidal dissipation, surface heat flow, and figure of viscoelastic models of Io. *Icarus* 75, 187-206.

Sigurdsson, H., and R. MacDonald 1999. Geologic history of the Soufriere St. Vincent Volcano. *Bull. Volcanol.*, in press.

Simkin, T. and L. Siebert 1994. *Volcanoes of the World*. Smithsonian Institution (2nd edition), Geoscience Press, Tucson.

Simonelli, D. P., Veverka, J., and A. S. McEwen 1997. Io: Galileo evidence for major variations in regolith properties. *Geophys. Res. Lett.* 24, 2475-2478.

Sinton, W. M. 1980. Io's 5-micron variability. *Icarus* 235, L49-51.

Smith, B. A., and the Voyager Imaging Team 1979. The Jupiter system through the eyes of Voyager 1. *Science* 204, 951-972.

Smythe, W. D., and 14 colleagues 1995. Galilean Satellite Observation Plans for the Near-Infrared Mapping Spectrometer on the Galileo Spacecraft. *J. Geophys. Res.* 100, 18,957-18,972.

Smythe, W. D., R. Lopes-Gautier, A. Davies, R. Carlson, L. Kamp, L. Soderblom, and the Galileo NIMS Team 1997. A temperature distribution map of Io from Galileo's Near-Infrared Mapping Spectrometer (NIMS). In *Io during the Galileo Era*, p. 14, Lowell Observatory, Flagstaff, AZ.

Smythe, W. D., R. Lopes-Gautier, L. Kamp, A. G. Davies, R. W. Carlson, L. A. Soderblom, and the Galileo NIMS Team 1999. Io Thermal Output Distribution from Galileo's Near-Infrared Mapping Spectrometer (NIMS). *Lunar Planet. Sci.* XXX (available on CD-Rom).

Spencer, J. R. and N. M. Schneider 1996. Io on the Eve of the Galileo Mission. *Annu. Rev. Earth Planet. Sci.* 24, 125-190.

Spencer, J. R., J. A. Stansberry, C. Dumas, D. Vakil, R. Pregler, and M. Hicks 1997a. A History of High-Temperature Io Volcanism, February 1995 to May 1997. *Geophys. Res. Lett.* 24, 2451-2454.

Spencer, J. R., A. S. McEwen, M. A. McGarth, P. Sartoretti, D. B. Nash, K.S. Noll, and D. Gilmore 1997b. Volcanic resurfacing of Io: Post-repair HST imaging. *Icarus* 127, 221-237.

Spencer, J. R., P. Sartoretti., G. E. Ballester, A. S. McEwen, J. T. Clarke, and M. McGarth 1997c. The Pele plume (Io): Observations with the Hubble Space Telescope. *Geophys. Res. Lett.* 24, 2471-2474.

Stansberry, J. A., J. R. Spencer, R. R. Howell, C. Dumas, and D.

Vakil 1997. Violent silicate volcanism on Io in 1996. *Geophys. Res. Lett.* **24**, 2455-2458.

Strom, R. G., N. M. Schneider, R. J. Terrile, A. F. Cook, and C. Hansen 1981. Volcanic eruptions on Io. *J. Geophys. Res.* **86**, 8593-8620.

Thomas, P. C., M. E. Davies, T. R. Colvin, J. Oberst, P. Schuster, G. Neukum, M. H. Carr, A. McEwen, G. Schubert, M. J. S. Belton, and the Galileo Imaging Team 1998. The Shape of Io from Galileo Limb Measurements. *Icarus* **135**, 175-180.

Veeder, G.J., D. L. Matson, T. V. Johnson, D. L. Blaney, and J. D. Goguen 1994. Io's heat flow from infrared radiometry: 1983-1993. *J. Geophys. Res.* **99**, 17,095-17,162.

Wooster, M. J. and D. A. Rothery 1997. Thermal modelling of Lascar volcano, Chile, using infrared data from the along-track scanning radiometer: a 1992-1995 time series. *Bull. Volcanol.* **58**, 566-579.

FIGURE CAPTIONS:

Figure 1. Top: Distribution of hot spots on Io, shown on a global mosaic made from Galileo SSI images. Hot spots marked in dark blue were detected by Galileo SSI and NIMS, hot spots marked in red were detected by ground-based telescopes. Bottom: Distribution of hot spots detected by Voyager IRIS, which had only a limited view of the surface of Io. The approximate coverage of Voyager IRIS observations is shown by the dashed lines (from Pearl and Sinton 1982).

Figure 2: Distribution of active volcanic centers (from Table 1) with latitude (above) and longitude (below). The dashed line represents the expected result for a uniform areal distribution of hot spots with latitude. The higher number of Voyager IRIS hot spots at high latitudes on the southern hemisphere than on the northern reflects the geometry of the Voyager fly-by.

Figure 3: Hot spots detected during five NIMS observations between orbits G2 and E4. All observations were taken in reflected sunlight. The 5-micrometer flux for individual hot spots is estimated by subtracting the 5-micrometer flux from a nearby "cold" pixel. The flux is plotted against the emission angle for each hot spot in order to assess the effect of viewing geometry. There is no clear correlation between number of hot spots detected and emission angle. The effect of emission angle is partly illustrated by the changes in the 5-micrometer brightness of Prometheus and Pele,

though it is likely that actual changes in the flux also took place.

Figure 4a: Distribution of active volcanic centers (from Table 1) plotted on the topographic map from Gaskell et al. [1988]. The contours are in 0.5 km intervals, from -2 km (darkest) to + 2 km (lightest).

Figure 4b: Comparison of distribution of active volcanic centers and area with elevation. Dashed line: relationship between area and elevation, from Gaskell et al. [1988]. Solid line: distribution of active volcanic centers with elevation.

Figure 5: Plots of distribution of active volcanic centers (from Table 1) plotted over the heat flow patterns predicted by Ross et al. [1990]. Top: Deep-mantle model. Bottom: Asthenosphere model. Heat flow contours in $W m^{-2}$.

Figure 6: Surface features associated with active volcanic centers. Images of Loki, Amaterasu, Babbar, Mbali, Karei, Daedalus, Pele, Pillan, Creidne, Acala, and Euboea are from Voyager, others are from Galileo SSI. Spatial resolution is 2 km/pixel in all cases. All are simple cylindrical projection, clear filter images.

Figure 7: Active volcanic centers (from Table 1) plotted on map of Io's major color units [from Geissler et al. 1998]. Black corresponds to low-albedo areas, dark grey to red/orange areas,

light grey to yellow/green areas and white to white/light grey areas. The imaging data used to make these maps has poorer resolution (and therefore more uncertainties) in the sub-Jovian hemisphere, centered on 0 degrees longitude. This uncertainty is probably responsible for hot spots between 0 and 60 degrees being consistently to the left of low-albedo areas.

Figure 8: Plot showing NIMS spatial resolution of the closest approach observation in each orbit against the number of hot spots detected in each of those observations.

Figure 9: The brightening of Loki during 1997 observed by NIMS during Galileo orbits E6 and G7. Loki is seen in daylight in E6, near the terminator in G7. Both maps are at 2.9564 micrometers. In E6, the signal from Loki at this wavelength is not significantly above the background, though the signal at wavelengths longer than 3.5 micrometers is. After the brightening, Loki can be seen clearly above the background in the 2.9564 map from the G7 observation.

Figure 10: Ground-based data by J. Spencer and colleagues (diamonds) show the variation in the 3.5 micrometer brightness of Loki from 1995 to 1997. NIMS observed Loki in darkness during orbit G7 and a single-temperature fit to the NIMS data (single asterisk) yields $T = 500 \text{ K}$, $\text{Area} = 1539 \text{ km}^2$, consistent with the trend seen by the ground-based observations.

Figure 11: Locations of hot spots plotted over the heat flow

patterns predicted by the asthenosphere model [Ross et al. 1990]. Persistent hot spots (filled orange circles) and active plumes (blue circles) are marked. Contours are in $W m^{-2}$. All persistent hot spots and active plumes are located within the $1 W m^{-2}$ regions and all are located at latitudes lower than 50 degrees.

Additional information:

R. Lopes-Gautier, W.D. Smythe, A.G. Davies, R.W. Carlson: JPL, MS
183-601, Pasadena, CA 91109 (rlopes@issac.jpl.nasa.gov,
agd@kookaburra.jpl.nasa.gov, rcarlson@issac.jpl.nasa.gov,
wsmythe@issac.jpl.nasa.gov).

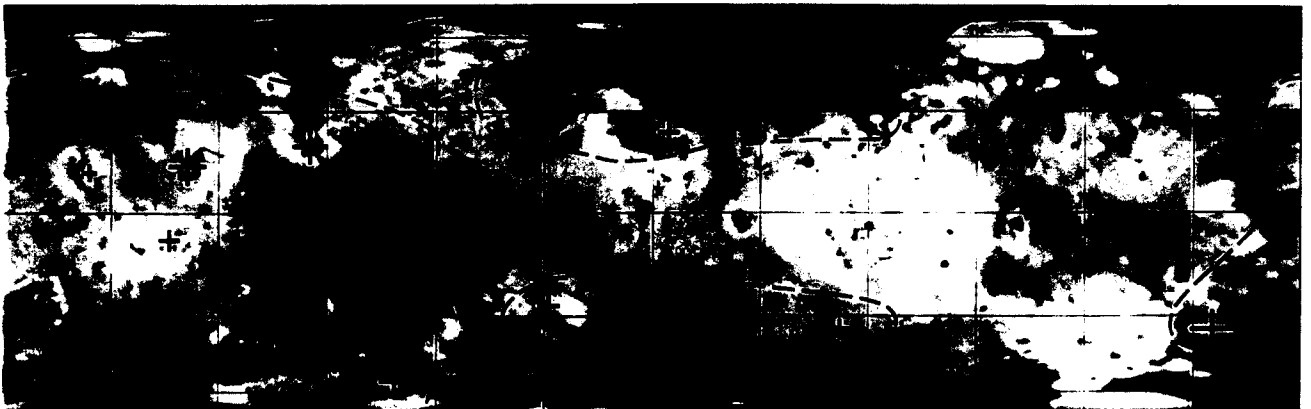
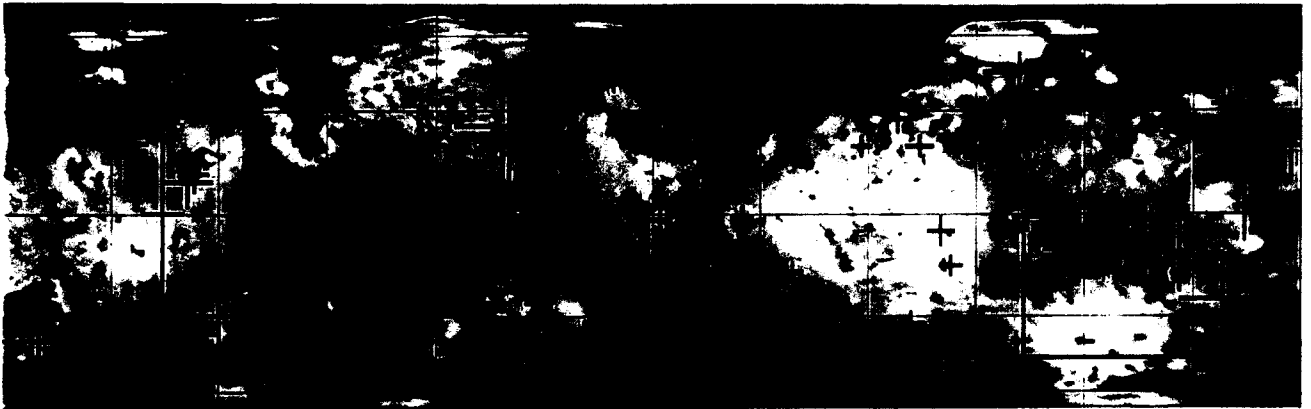
A.S. McEwen, P. Geissler, Department of Planetary Sciences, Lunar
and Planetary Laboratory, University of Arizona, P.O. Box 210092,
Tucson, AZ 85721-0092 (mcewen@pir1.lpl.arizona.edu,
geissler@pir1.lpl.arizona.edu)

L. Kamp: JPL, MS 168-514, Pasadena, CA 91109
(kamp@issac.jpl.nasa.gov).

F.E. Leader and R. Mehlman, Institute of Geophysics and Planetary
Physics, University of California, Los Angeles, CA 90095
(fleader@igpp.ucla.edu, rmehlman@igpp.ucla.edu).

L. Soderblom, Branch of Astrogeologic Studies, U.S. Geological
Survey, Flagstaff, AZ 86001 (lsoderblom@flagmail.wr.usgs.gov).

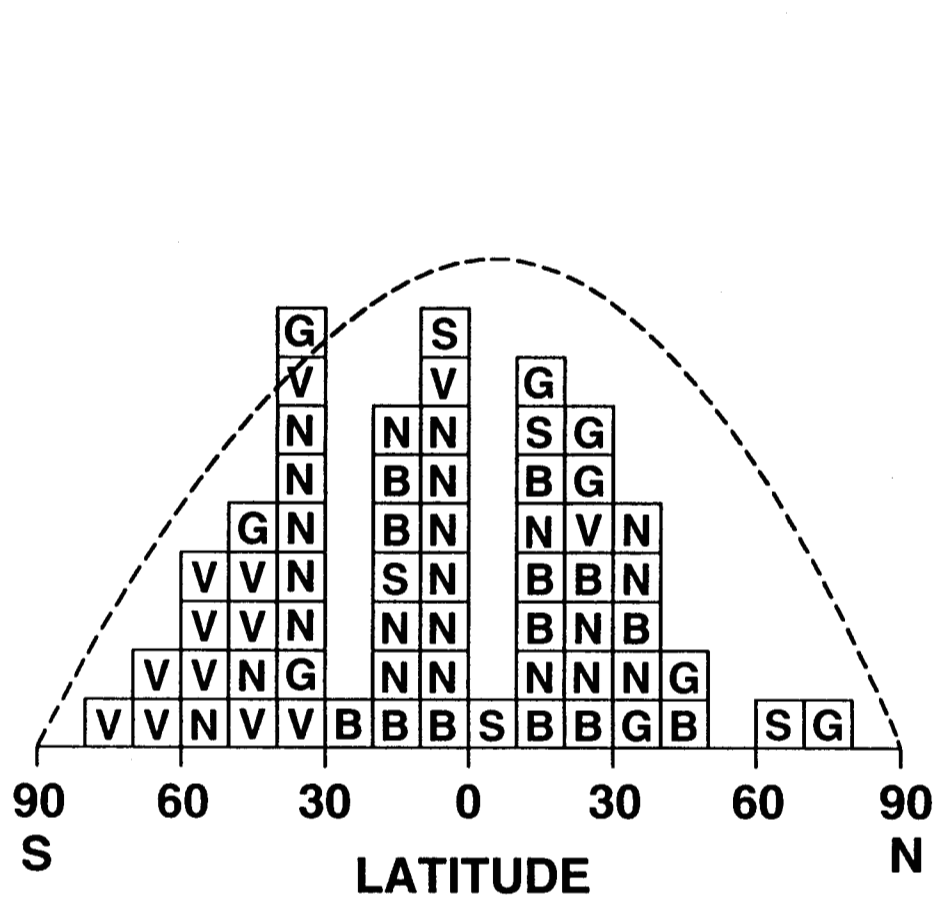
(color)



0 330 300 270 240 210 180 150 120 90 60 30 0

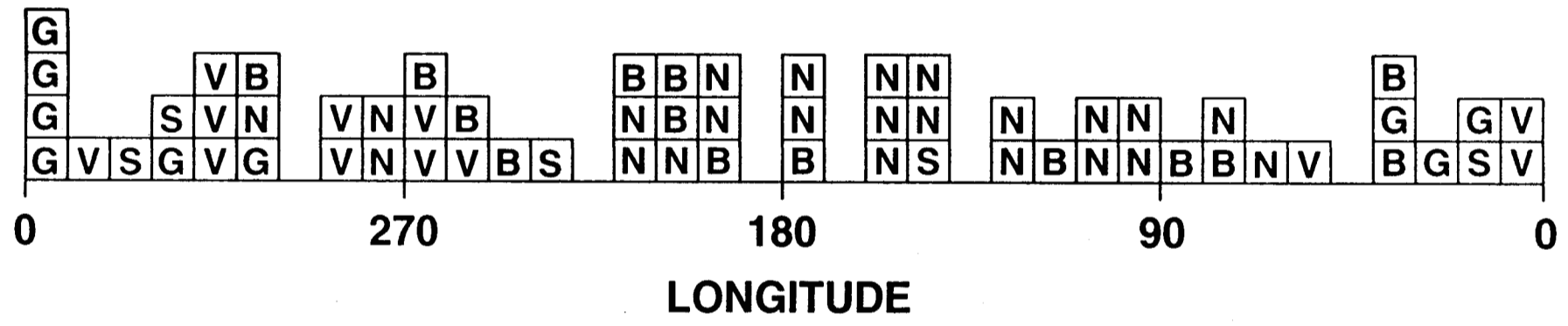
figure 1

FIG 2



DETECTIONS

- N** NIMS ONLY
- S** SSI ONLY
- B** DETECTED BY BOTH NIMS AND SSI
- V** DETECTED BY VOYAGER IRIS ONLY
- G** DETECTED FROM GROUND-BASED OBSERVATIONS



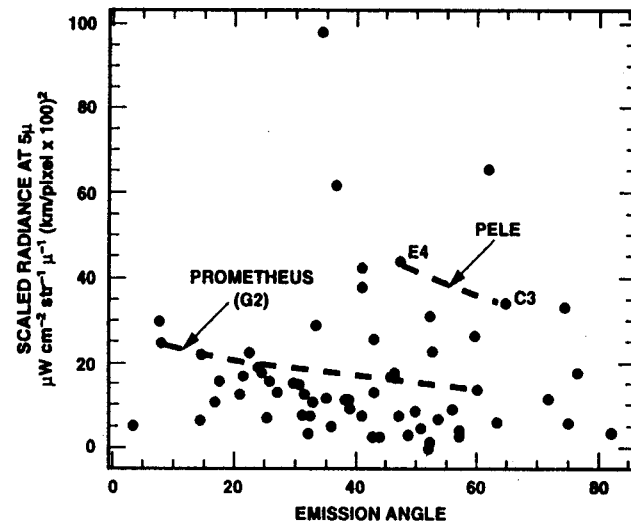
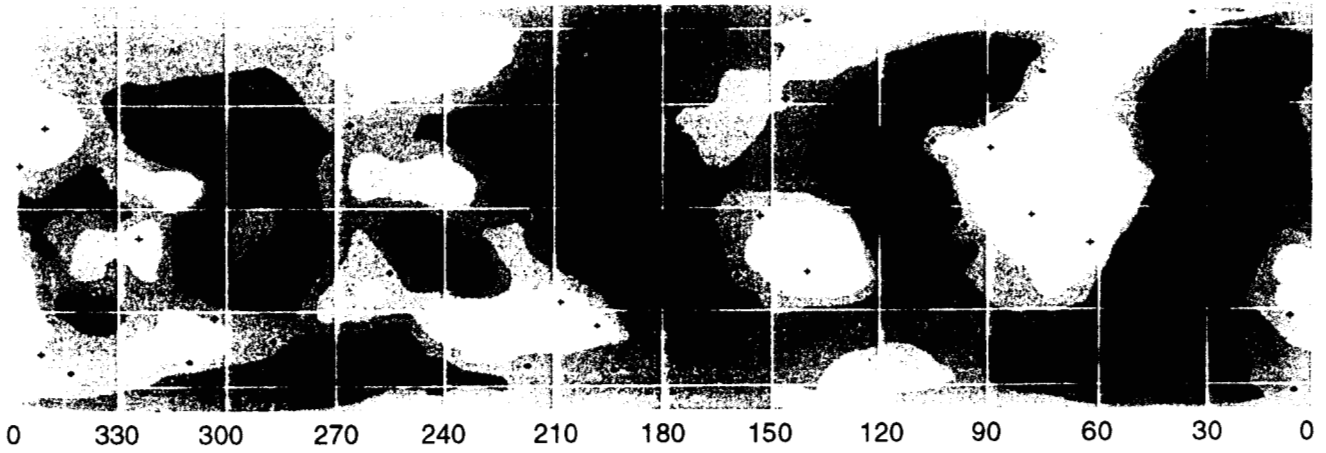


Figure 3

(color)



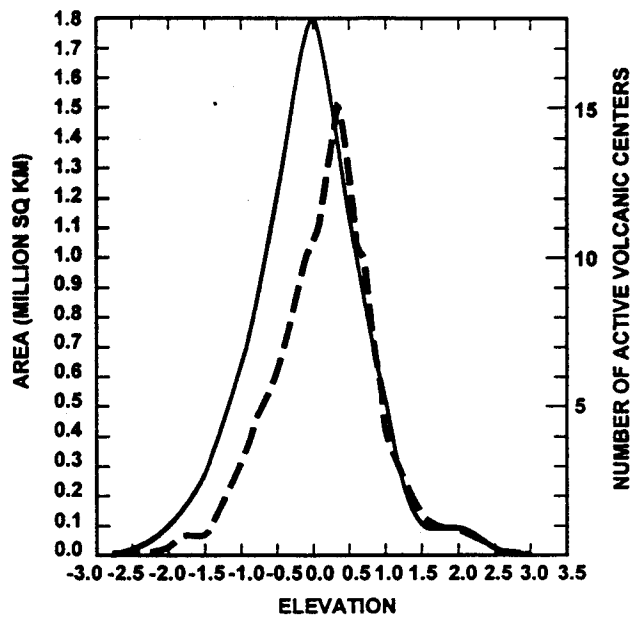


Figure 4b

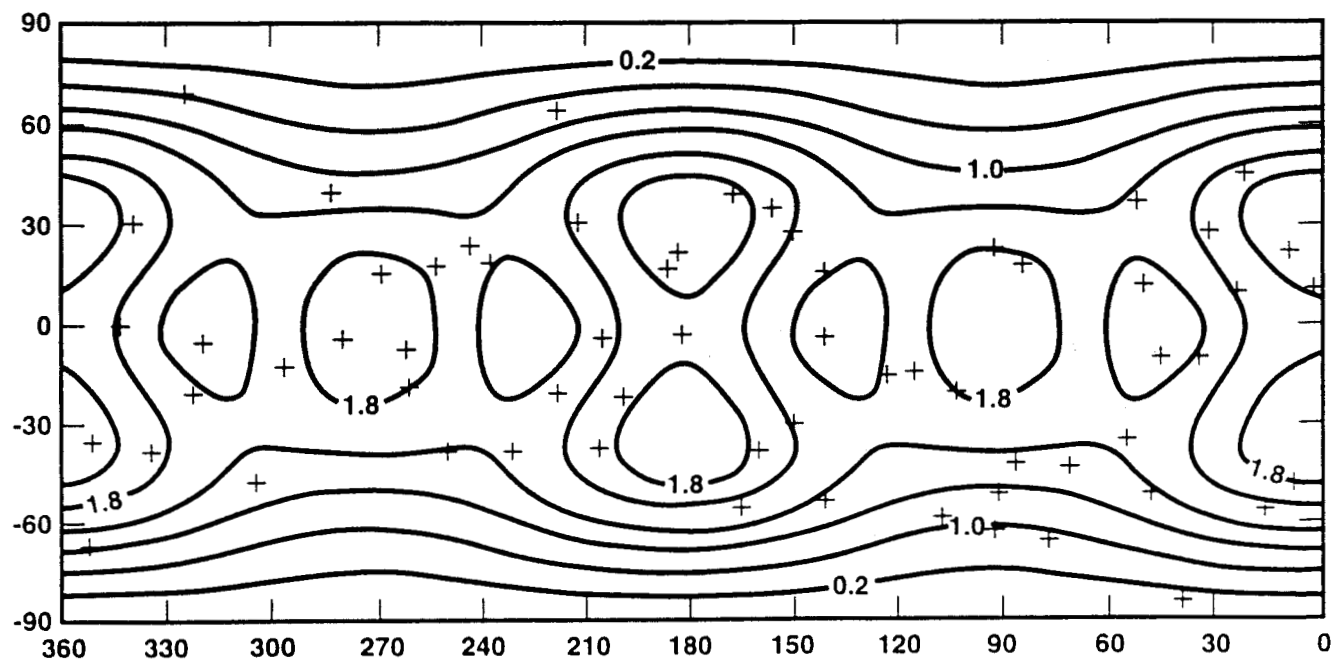
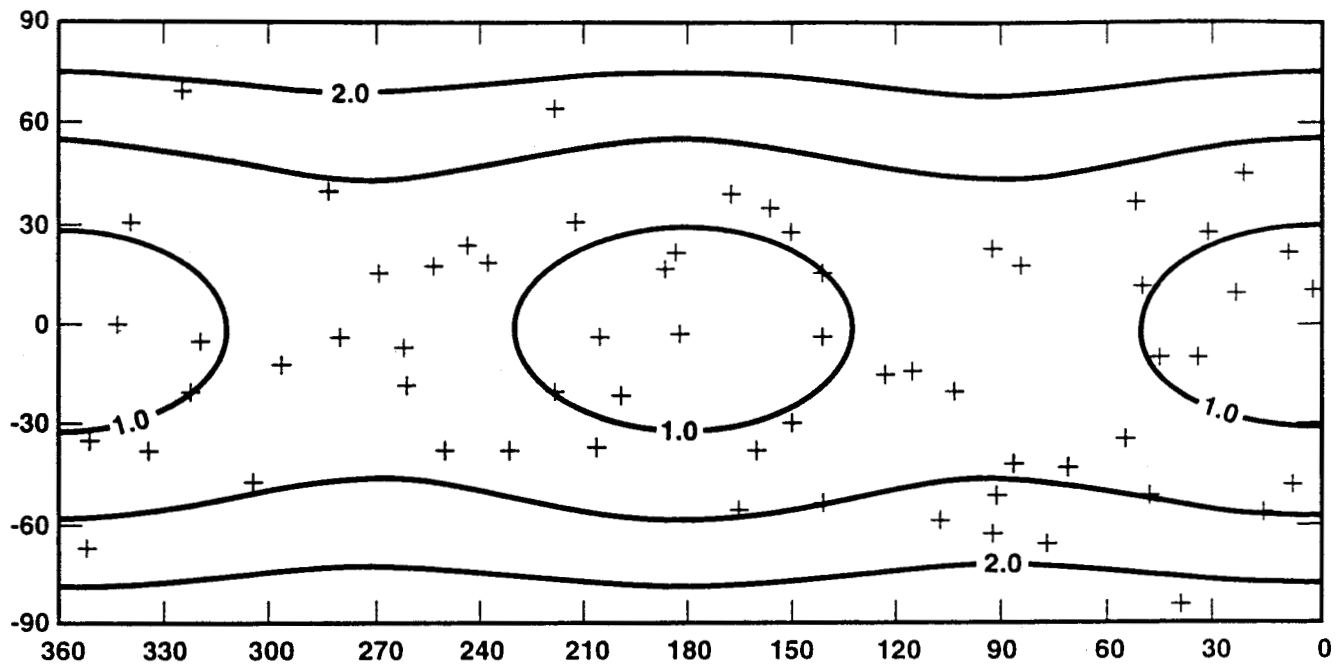
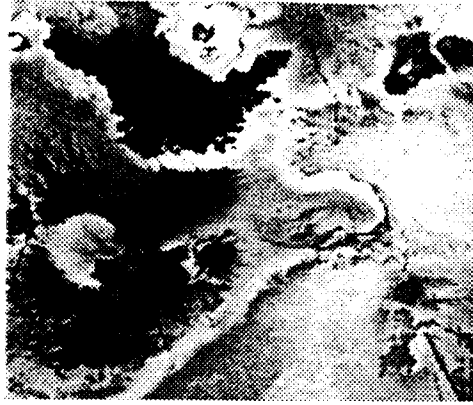


Figure 5a, 5b



(a) Amaterasu



(c) Lei-Kung, Fo, Isum



(d) Volund, Zamama



(f) Dusura, Maui, Amirani



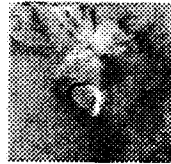
(b) Daedalus



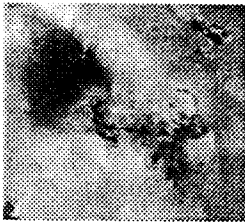
(e) Gish Bar



(g) Pele



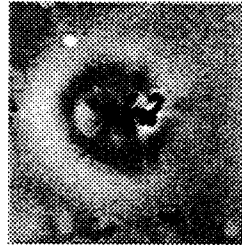
(h) Pillan



(i) Acala



(j) Culaan



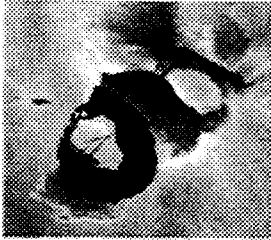
(k) Prometheus



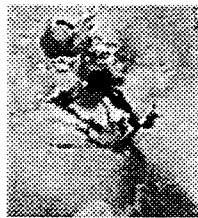
(l) Sigurd (top)



(m) Hi'iaka



(n) Loki



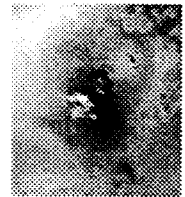
(o) Marduk



(p) Shamash



(q) Tupan



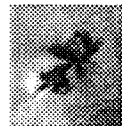
(r) Karei



(s) Euboea



(t) Malik



(u) Mbali



(v) Creidne

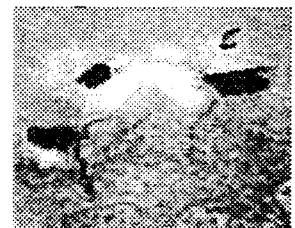


(w) Ulgen, Babbar, Svarog

100 km

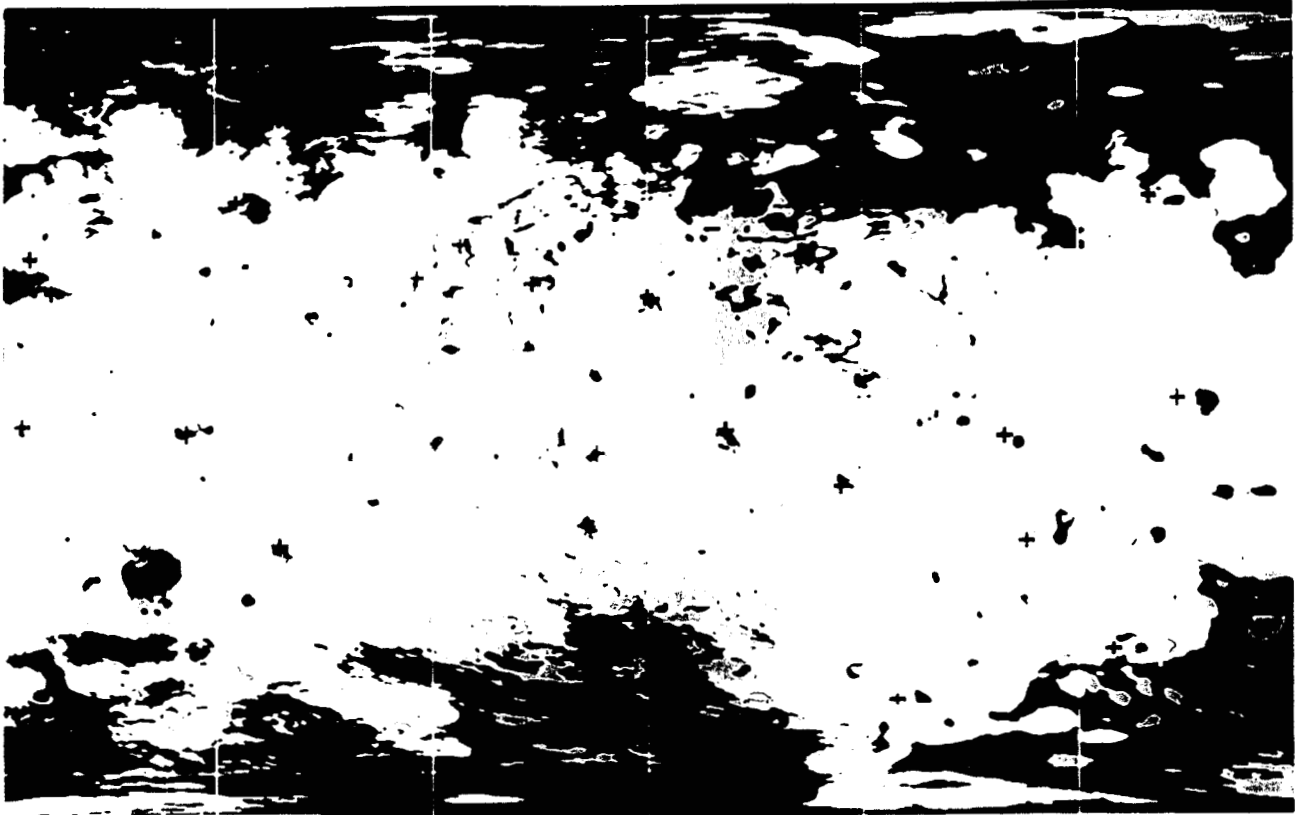


(x) Kurdalagon

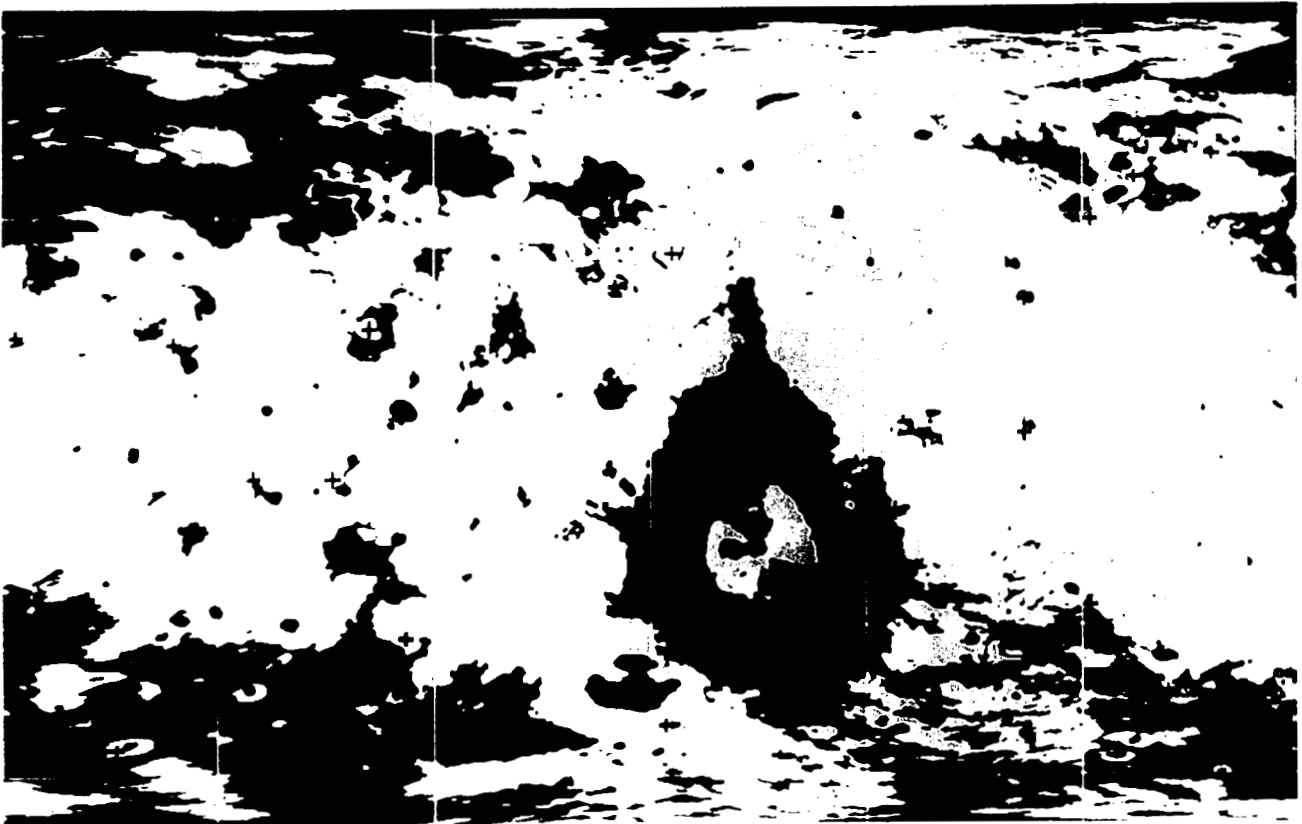


(y) Sethlaus (right)

(color)



180 150 120 90 60 30 0



0 330 300 270 240 210 180

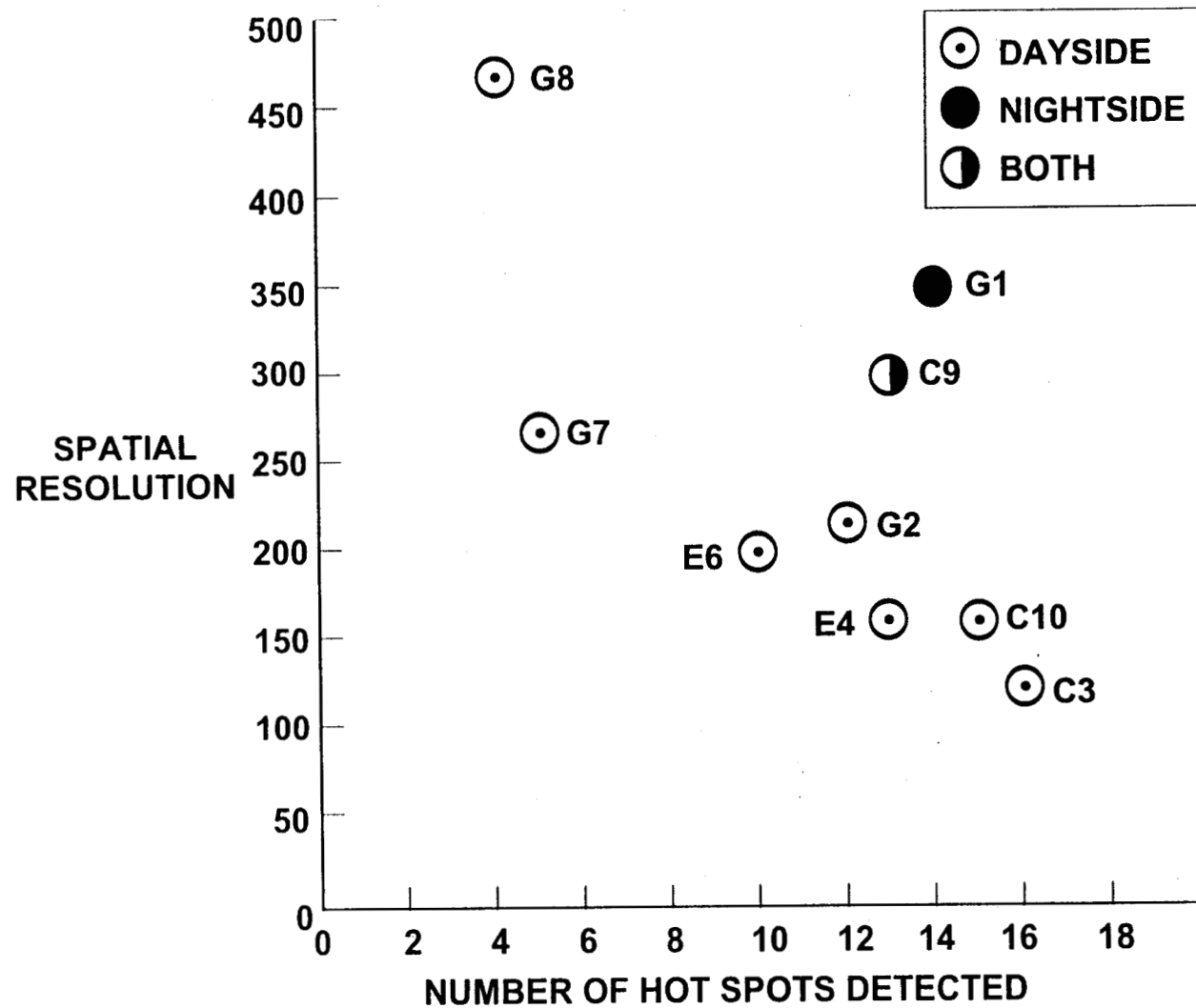


Figure 8

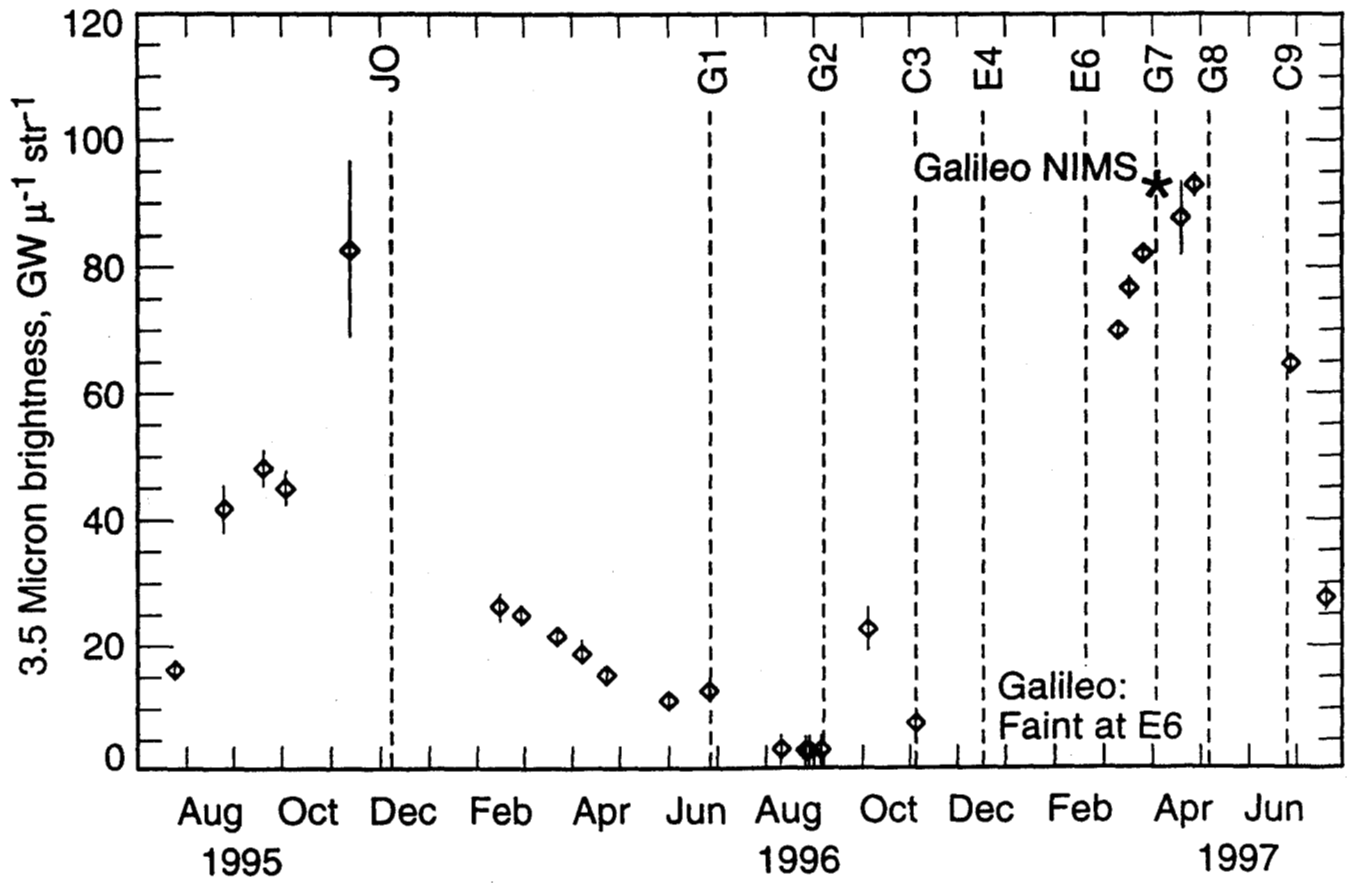


Figure 10

